



Deposited via The University of Sheffield.

White Rose Research Online URL for this paper:

<https://eprints.whiterose.ac.uk/id/eprint/145784/>

Version: Accepted Version

Article:

Adams, K.D. and Rhodes, E.J. (2019) Late Pleistocene to present lake-level fluctuations at Pyramid and Winnemucca lakes, Nevada, USA. *Quaternary Research*, 92 (1). pp. 146-164. ISSN: 0033-5894

<https://doi.org/10.1017/qua.2018.134>

This article has been published in a revised form in *Quaternary Research* [<http://doi.org/10.1017/qua.2018.134>]. This version is free to view and download for private research and study only. Not for re-distribution, re-sale or use in derivative works. © University of Washington.

Reuse

This article is distributed under the terms of the Creative Commons Attribution-NonCommercial-NoDerivs (CC BY-NC-ND) licence. This licence only allows you to download this work and share it with others as long as you credit the authors, but you can't change the article in any way or use it commercially. More information and the full terms of the licence here: <https://creativecommons.org/licenses/>

Takedown

If you consider content in White Rose Research Online to be in breach of UK law, please notify us by emailing eprints@whiterose.ac.uk including the URL of the record and the reason for the withdrawal request.

1 Late Pleistocene to present lake-level fluctuations at Pyramid and Winnemucca lakes, Nevada,

2 USA

3

4 Kenneth D. Adams*

5 Desert Research Institute

6 2215 Raggio Parkway

7 Reno, NV 89512

8 USA

9 (775) 673-7345

10 kadams@dri.edu

11

12 Edward J. Rhodes

13 Department of Geography

14 University of Sheffield,

15 Sheffield, S10 2TN

16 United Kingdom

17

18

19

20 *Corresponding author

21

22 **ABSTRACT**

23 A new lake-level curve for Pyramid and Winnemucca lakes, NV is presented that indicates that
24 after the ~15,500 cal yr BP Lake Lahontan highstand (1338 m), lake level fell to an elevation
25 below 1200 m, before rising to 1230 m at the 12,000 cal yr BP Younger Dryas highstand. Lake
26 level then fell to 1155 m by ~10,500 cal yr BP followed by a rise to 1200 m around 8000 cal yr
27 BP. During the mid-Holocene levels were relatively low (~1155 m) before rising to moderate
28 levels (1190 – 1195 m) during the neopluvial period (~4800 – 3400 cal yr BP). Lake level again
29 plunged to about 1155 m during the Late Holocene Dry Period (~2800 – 1900 cal yr BP) before
30 rising to about 1190 m by ~1200 cal yr BP. Levels have since fluctuated within the elevation
31 range of about 1170 – 1182 m except for the last 100 years of managed river discharge when
32 they dropped to as low as 1153 m. Late Holocene lake-level changes correspond to volume
33 changes between 25 and 55 km³ and surface area changes between 450 and 900 km². These lake
34 state changes probably encompass the hydrologic variability possible under current climate
35 boundary conditions.

36

37 **Keywords:** Lake Lahontan, Pyramid Lake, Winnemucca Lake, Pleistocene, Holocene

38

39 **INTRODUCTION**

40 The Great Basin of the western U.S. contained more than 60 pluvial lakes during the late
41 Pleistocene (e.g., Smith and Street-Perrot, 1983; Benson and Thompson, 1987; Morrison, 1991;
42 Negrini, 2002; Reheis et al., 2014). Lake levels in each of these basins fluctuated according to
43 prevailing climate conditions in their respective drainage basins. By the end of the Pleistocene,
44 however, most of these lakes were greatly diminished from their late Pleistocene highstands of

45 just a few thousand years before or had completely evaporated. Only a handful of these basins
46 contained lakes during the Holocene and fewer still maintained lakes into the historical period.

47 Pyramid Lake in western Nevada is the third largest perennial lake in the Great Basin today,
48 behind Great Salt Lake and Lake Tahoe, and represents a remnant of pluvial Lake Lahontan that
49 has existed throughout the Holocene and into the historical period (Fig. 1) (Benson and
50 Thompson, 1987). Its sister basin, Winnemucca Lake, is located directly to the east and also
51 contained a relatively large lake in the early historical period (Russell, 1885; Hardman and
52 Venstrom, 1941; Harding, 1965) and at other discrete times during the Holocene (Hattori, 1982;
53 Hattori and Tuohy, 1993), but is currently dry due to upstream water diversions. These two
54 terminal basins are connected by a low sill (Mud Lake Slough; ~1178.5 m) so can be thought of
55 as the same lake system when lake levels were moderately high (Fig. 2).

56 This combined lake system likely has preserved a continuous record of climate change from
57 the Pleistocene to the modern era that reflects changing conditions within its watershed that
58 includes Lake Tahoe and the northern Sierra Nevada (Fig. 1). Although Pyramid and
59 Winnemucca lakes reside in Nevada, deciphering their past lake-level fluctuations is highly
60 relevant for understanding long term water-supply fluctuations in northern California as well
61 because most of the water for these lakes is derived from near the crest of the Sierra Nevada.
62 Therefore, the aim of this paper is to present a well-constrained lake-level curve for Pyramid and
63 Winnemucca lakes that is based on dated shorelines and other indicators of changing lake levels
64 over the last 16,000 years, from the time of the Lake Lahontan highstand to the present. The
65 emphasis, however, is placed on the late Holocene part of the record because this information is
66 important for defining natural hydrologic variability that is possible under modern and future
67 climatic conditions.

68

69 **GEOLOGIC SETTING, CLIMATE, AND HYDROLOGY**

70 Pyramid and Winnemucca basins are located at the terminus of the Truckee River, whose
71 headwaters are Lake Tahoe and other tributaries draining the Sierra Nevada crest (Fig. 1). This
72 river is the only significant source of inflow to Pyramid and Winnemucca lakes on a volumetric
73 basis. The drainage basin encompasses about 7050 km² and most of the flow in the river is
74 derived from the highest parts of the basin (> 2500 m) where mean annual precipitation ranges
75 from about 150 to 170 cm/yr (Daly et al., 2008), falling mostly as snow in the winter months that
76 subsequently melts in the spring (Fig. 1). Precipitation at Pyramid Lake (~1160 m) is much less
77 and ranges from about 16 to 20 cm/yr (Daly et al., 2008). In contrast, mean annual lake
78 evaporation at Pyramid Lake is reported to average about 125-135 cm/yr (Houghton et al., 1975;
79 Milne, 1987).

80 Flows down the Truckee River during spring snowmelt typically range from 60 to 120 m³s⁻¹
81 but over the last 100 years or so large floods of >300 m³s⁻¹ have occurred every 10 or 20 years
82 due to heavy rains or rain-on-snow events (Horton, 1997; Adams, 2012a). In terms of flow
83 volumes, the mean annual natural flow of the Truckee over the last 100 years is about 0.67 km³,
84 ranging from 2.2 km³ (1983) to 0.16 km³ (1931) (Fig. 3) (Data accessed Dec. 17, 2017 from
85 USGS gage 10346000, Truckee River at Farad). The Truckee delivered about 1.7 km³ of water to
86 Pyramid Lake during the 2017 water year (WY), leading to a lake level rise of about 3 m from an
87 historically wet winter (Fig. 4). Because all of the upstream reservoirs on the Truckee River were
88 at very low levels at the beginning of the 2017 WY, due to drought (WY 2011-2015), the total
89 water delivered to Pyramid Lake in 2017 may have exceeded the 1983 volume, if there were no
90 upstream impoundments or diversions.

91 The Pyramid and Winnemucca basins straddle the boundary between the primarily right-
92 oblique Walker Lane belt to the west (Stewart, 1988; Wesnousky, 2005) and the Basin and
93 Range Province to the east, which is characterized more by east-west directed extension
94 (Stewart, 1978; Unruh et al., 2003). The Virginia Mountains and Pah Rah Range, to the west and
95 southwest of Pyramid Lake, respectively (Fig. 2), are primarily composed of Tertiary volcanic
96 rocks, as is the Lake Range that separates the Pyramid and Winnemucca basins (Bonham and
97 Papke, 1969). The Nightingale Range to the east of Winnemucca Lake is composed of Mesozoic
98 metasedimentary rocks and younger Mesozoic granitics, overlain in places by Tertiary volcanic
99 rocks (Van Buer, 2012).

100

101 **PREVIOUS WORK**

102 Early historical lake-level fluctuations at Pyramid and Winnemucca lakes, prior to large-scale
103 diversions, provide a frame of reference for the magnitude of Holocene fluctuations. Russell
104 (1885) produced detailed maps of the hydrography of these basins that show how large the water
105 bodies were in 1882. At that time, Pyramid Lake was at an elevation of about 1178 m and
106 Winnemucca Lake was at about 1175 m (Hardman and Venstrom, 1941; Harding, 1965).
107 Pyramid Lake had reached its historical highstand elevation of about 1182 m in 1862, 1868, and
108 again in 1891 after exceptionally wet winters in those years (Fig. 4) (Hardman and Venstrom,
109 1941). Lake level remained relatively high until about 1913 although substantial diversions of
110 Truckee River flow into the Carson River basin began in 1906 via Derby Dam and the Truckee
111 River canal (Horton, 1997). Winnemucca Lake was dry in the 1840s but rose rapidly to its
112 historical highstand of about 1175 m in 1882 and again in 1890 (Fig. 4). The diversion of
113 Truckee River water by Derby Dam ultimately caused the level of Pyramid Lake to drop and led

114 to incision in the distal part of the Truckee River due to lowered base level and abandonment of
115 Mud Lake Slough (Hardman and Venstrom, 1941; Harding, 1965; Adams, 2012a). This incision
116 cut the main water supply for Winnemucca Lake causing it to completely evaporate by the mid-
117 1930s (Harding, 1965).

118 The first radiocarbon chronology for the Lahontan basin was produced by Broecker and Orr
119 (1958), which was subsequently added to by Broecker and Kaufman (1965). Although these
120 assessments include a handful of radiocarbon ages dating to the Holocene, they are not used in
121 the lake-level reconstructions presented herein because the shell samples were collected from
122 elevations below the historical highstand and radiocarbon ages generated in the early 1960s from
123 tufa are not thought to be reliable (e.g., Benson, 1978). The remaining Holocene ages from
124 Broecker and Orr (1958) were generated on organic carbon from archaeological sites that are
125 located far above maximum Holocene levels in the Pyramid and Winnemucca basins.

126 Born (1972) collected a series of wood radiocarbon samples from Truckee River delta
127 exposures that date from the Holocene. Although all of these samples were collected from below
128 the elevation of the historical highstand (~1182 m), some of them were collected from outcrops
129 of stream alluvium interbedded with lacustrine deposits, indicating times when lake level was
130 relatively low. Based on the ages and elevations of samples, as well as their depositional
131 environments, Born (1972) constructed a lake-level curve that shows relatively high lake levels
132 (≤ 1220 m) around 10,000 ^{14}C yr BP that descend to low levels between 8000 and 4000 ^{14}C yr
133 BP, and subsequent rises around 3000 ^{14}C yr BP and in the last few hundred years. Several
134 radiocarbon ages generated from wood samples collected by Prokopovich (1983) in the same
135 area are consistent with the lake-level interpretations presented by Born (1972).

136 Benson et al. (1992) presented a model for lake-level fluctuations at Pyramid Lake for the
137 late Pleistocene-Holocene transition. The model includes a highstand of about 1222 m at about
138 10,700 ¹⁴C yr BP that they correlated to the Younger Dryas (YD) period, which was followed by
139 a drop in lake level to about 1154 m by 9700 ¹⁴C yr BP, constrained by the age of sagebrush bark
140 cordage found at the north end of Pyramid Lake (Touhy, 1988). Briggs et al. (2005) dated an
141 articulated mussel shell to 10,800 ¹⁴C yr BP, which was collected from a beach ridge at 1212 m.
142 Although this age and elevation is consistent with the curve of Benson et al. (1992), Briggs et al.
143 (2005) presented geomorphic and stratigraphic evidence that the YD highstand actually
144 transgressed to an elevation of about 1230 m. Briggs et al. (2005) also dated beach ridges at 1187
145 m and 1195 m to about 3600 ¹⁴C yr BP and 2600 ¹⁴C yr BP, respectively. These dated shorelines
146 indicate that late Holocene Pyramid levels fluctuated with much higher amplitude than suggested
147 by Born (1972).

148 Hattori (1982) and Hattori and Tuohy (1993) used the ages of cultural materials found at
149 archaeological sites at the north end of Winnemucca Lake to infer the periods during the
150 Holocene when a lake was present there. This inference was based on the lack of other water
151 sources available to the inhabitants of those sites and the type of materials found, which showed
152 a dependence on marsh or lake resources (Hattori and Tuohy, 1993). Their data show relatively
153 high frequencies of radiocarbon ages between 4000 – 3500 ¹⁴C yr BP and 2500 – 1000 ¹⁴C yr
154 BP.

155 Benson et al. (2002) documented the frequency and durations of hydrologic fluctuations at
156 Pyramid Lake over the last 7600 cal yr BP using a variety of core proxies and regional
157 paleoclimatic data. They found that multiple multi-decadal to multi-centennial droughts have
158 affected this region throughout the mid to late Holocene. The higher temporal resolution of these

159 core records over typical outcrop and landform records provide important information about the
160 timing of hydrologic changes, but cannot be used directly to infer the magnitude of lake level or
161 volume changes (Benson et al., 2002).

162 Adams et al. (2008) synthesized the available information on the post-highstand history of
163 Pyramid and Winnemucca lakes and also compared the ages and elevations of archaeological
164 sites to the lake-level records in order to test the hypothesis that lake-level changes influenced
165 the spatio-temporal distribution of archaeological sites. This compilation of geological and
166 archaeological data focused on the period from the Lahontan highstand to the beginning of the
167 middle Holocene (~15,500 – 7000 cal yr BP), which includes the YD period. Based on available
168 evidence at that time, Adams et al. (2008) concluded that during the YD, lake level reached an
169 elevation of about 1230 m in the Pyramid and Winnemucca basins.

170 Benson et al. (2013a) presented a synthesis of paleoclimatic data for Pyramid Lake from the
171 period 48,000 to 11,500 cal yr BP, based on the ages of tufa samples at different elevations and
172 various core proxies. This latest effort represents the continuing evolution of lake-level curves of
173 Benson (1978), Thompson et al. (1986), Benson and Thompson (1987), and Benson et al. (1995).
174 The curve of Benson et al. (2013a) was further modified by Benson et al. (2013b) for the period
175 14,000 to 9000 cal yr BP by incorporating the ages of tufa on which petroglyphs were carved. A
176 slight variation on the curve of Benson et al. (2013a) was also made by Reheis et al. (2014) for
177 the period 16,000 to 10,000 cal yr BP, by incorporating the ages and depositional settings of
178 organic carbon samples and tephra beds to constrain the level of Lake Lahontan at specific times.

179

180 **METHODS**

181 To better understand the history of post-highstand lake-level fluctuations in the Pyramid and
182 Winnemucca basins we evaluated and selectively used existing geochronologic data, created
183 detailed geomorphic maps, surveyed the elevations of key features, described natural and
184 artificial exposures through lake deposits, and collected and processed radiocarbon and
185 luminescence dating samples. Standard field and laboratory procedures were utilized in each of
186 these tasks as outlined below.

187 Geochronologic data were initially compiled from numerous published sources and evaluated
188 for their quality and context. Of the hundreds of radiocarbon ages that pertain to lake-level
189 fluctuations in the Pyramid and Winnemucca basins (e.g., Broecker and Orr, 1958; Broecker and
190 Kaufman, 1965; Born, 1972; Benson, 1978; Benson et al., 1990, 1992, 1995, 2002, 2013a,b;
191 Thompson et al., 1986; Adams and Wesnousky, 1998; Bell et al., 2005a; Briggs et al., 2005;
192 Adams et al., 2008), only a relatively small percentage of these are related to post-highstand
193 lake-level fluctuations. Radiocarbon ages have been generated on a variety of materials including
194 charcoal, wood, plant debris, bone, shells, tufa, total organic fraction of sediments, and bulk
195 organic content of soils that were subjected to a variety of pretreatment techniques. In addition,
196 many ages have been generated from archaeological contexts (e.g., Hattori, 1982; Hattori and
197 Tuohy, 1993; Adams et al., 2008) that span a range of elevations.

198 Samples were classified by whether they were deposited above, at or below lake level based
199 on their depositional setting using the guidance of Adams (2007, 2010) and Reheis et al. (2014).
200 Tufa ages from Broecker and Orr (1958) and Broecker and Kaufman (1965) were not used
201 because of their potential for contamination (e.g., Benson, 1978). The five Holocene tufa ages
202 from Benson et al. (1992) were also not used because they were all collected from elevations
203 below the historic highstand of Pyramid Lake. The potential reservoir effect in Pyramid Lake

204 was estimated to range from 200 and 600 years, depending on the size of the lake (Broecker and
205 Kaufman, 1958; Benson et al., 2002, 2013b), so all ages from shell or other carbonates are
206 considered maximum ages. All radiocarbon ages have been calibrated with the Calib 7.1
207 program using the IntCal13 calibration curve (Reimer et al., 2013) and are reported in
208 radiocarbon years before present (^{14}C yr BP) and calibrated years before present (cal yr BP).

209 Different kinds of landforms and sediments rimming the Pyramid and Winnemucca basins
210 record past lake-level fluctuations and their ages and elevations are used to reconstruct this
211 history. Detailed geomorphic mapping (1:5000-scale) of shorelines and related features at the
212 north end of Winnemucca Lake improved upon the mapping of Adams et al. (2008) and was
213 augmented with stratigraphic descriptions of key outcrops following the approach of Adams and
214 Wesnousky (1998) and Adams (2007, 2010). Radiocarbon samples were collected from beach
215 deposits that closely reflect particular lake levels.

216 We also employed Infrared stimulated luminescence (IRSL) dating to directly date samples
217 collected from the suite of beach ridges at the north end of Winnemucca Lake. Two samples
218 each were collected from six beach ridges ranging in elevation from 1177 – 1231 m. Five
219 samples were collected from two different exposures on the 1202 m beach ridge (Table 2). All
220 samples were collected by pounding a steel pipe horizontally into the vertical wall of a trench or
221 pit and then excavating the pipe without exposing the sediment to light and capping the ends
222 with light-tight material. An attempt was made to sample parts of the exposures with visible
223 bedding in order to minimize the mixing effects of bioturbation, but no bedding was observed in
224 the excavations in the 1202 m ridge. In situ gamma spectrometer measurements were collected
225 from the same holes where the sediment was collected to determine dose rate. In addition, bulk
226 samples surrounding each sample site were collected for laboratory radiation measurements. All

227 samples were processed at the University of California, Los Angeles (UCLA) luminescence
228 laboratory using the single grain K-feldspar post IR IRSL protocol outlined in Rhodes (2015).
229 More details on this methodology are found in the supplementary data.

230 Stream terraces and fluvial deposits at a range of elevations along the lower Truckee River
231 represent different lake levels to which the river was graded, because Pyramid Lake acts as base
232 level for this system. Adams (2012a) showed that the Truckee River responds very quickly
233 (decadal time periods) to the lowering of Pyramid Lake by adjusting its slope through incision
234 and altering its planform. Therefore, elevations of the downstream extents of Holocene fluvial
235 terraces and deposits mapped by Bell et al. (2005a) are used as close approximations of lake
236 level when these terrace surfaces represented the active floodplain of the Truckee River graded
237 to Pyramid Lake.

238 Elevations associated with dating samples and landforms either were surveyed with a total
239 station referenced to local geodetic benchmarks or a map-grade GPS instrument with differential
240 correction, or were determined from high precision LiDAR topographic data. All elevations
241 therefore have a precision of ≤ 1 m, and sometimes are substantially more precise, which is well
242 within the natural variability in the height that shorelines form above an associated still water
243 plane (Atwood, 1994; Adams and Wesnousky, 1998). Exceptions to this level of precision
244 include the radiocarbon samples of Born (1972) and Prokopovich (1983) from the Truckee River
245 delta, but these were collected from below the elevation of the historical highstand and only
246 provide broad limiting elevations on lake-level fluctuations. Elevations are reported as meters
247 above sea level (MASL) (NAVD88), which is shortened to meters (m). The horizontal
248 coordinate system is UTM NAD 83 Zone 11.

249 To assess the paleohydrologic implications of Holocene lake-level fluctuations, the
250 hypsometries of the subaerial portions of the Pyramid and Winnemucca basins were calculated
251 from 10 m DEMs using the surface volume tool in ArcGIS®. The hypsometry of the submerged
252 portion of Pyramid was derived from the bathymetric data set of Eisses et al. (2015), which was
253 then integrated with the results calculated from the subaerial 10 m DEM data.

254

255 **RESULTS**

256 The history of lake-level fluctuations in the Pyramid and Winnemucca basins is reconstructed
257 from multiple lines of evidence that include the ages and elevations of shorelines surrounding the
258 basins, fluvial terraces and deposits graded to former lake levels, pack rat middens that have not
259 been submerged since their formation, and archaeological materials found at low elevations
260 surrounding the basins (Table 1). This history is also constrained by the elevations of both
261 internal and external sills, where water spilling to a downstream basin effectively restricts further
262 lake-level rises until the downstream basin fills to the elevation of the sill.

263

264 **Topographic constraints**

265 The two sills that affected lake-level fluctuations in the Pyramid and Winnemucca basins during
266 the Holocene include Mud Lake Slough, which constrains flow into Winnemucca Lake, and
267 Emerson Pass where spill into Smoke Creek Desert occurred (Fig. 2). When Russell was
268 working in the basin in the early 1880s, the Truckee River bifurcated near its distal end and one
269 branch of the river flowed through Mud Lake Slough and into Winnemucca Lake, while the
270 other branch continued into Pyramid Lake. According to historical records, the bifurcation of the
271 Truckee was not a permanent condition and the Mud Lake Slough channel was variously

272 occupied and abandoned by the Truckee River (Hardman and Venstrom, 1941). Based on a
273 detailed contour map of the area of bifurcation, Hardman and Venstrom (1941) determined that
274 the elevation of the junction of the two channels was about 1177.5 m, which is similar to the
275 LiDAR-derived elevation of 1178.5 m. From the junction, the low gradient channel (~0.0003
276 m/m) of Mud Lake Slough extends about 13 km to the north where it becomes unconfined and
277 deposits from the channel spread out into a broad, delta-like feature covering the southern end of
278 the Winnemucca Lake bed (Fig. 2).

279 When Pyramid Lake was at or above 1178.5 m, the Truckee River-Mud Lake Slough
280 junction acted as a sill and water from Pyramid flowed toward Winnemucca Lake (Russell,
281 1885; Hardman and Venstrom, 1941). At no time in the late 19th century, however, were the two
282 lakes at the same elevation (Fig. 4), despite Pyramid rising several times to inundate sill by
283 several meters (Hardman and Venstrom, 1941). These observations beg the question: how can
284 Pyramid rise to its historical highstand of about 1182 m, thereby submerging the sill by about 3.5
285 m, while Winnemucca only rose to its historical highstand of about 1175 m during the late 19th
286 century?

287 One potential explanation is the presence and elevation of a sand dune complex that blocks
288 the Mud Lake Slough channel about 11 km downstream from its junction with the Truckee River
289 (Fig. 5). These active transverse dunes terminate in the Mud Lake Slough channel and appear to
290 be sourced from sandy beach ridges on the southeast shore of Pyramid Lake, about 3.5 km to the
291 west-southwest of the blockage. The dunes are about 7 - 8 m thick where they block the channel
292 and the lowest point at the blockage is presently at about 1182 m, similar to the historical
293 highstand elevation of Pyramid Lake. Thus, the dunes may have effectively dammed the channel
294 at this elevation.

295 The other factor in the disparate lake levels is the evaporative potential and volume of
296 Winnemucca Lake below 1182 m (Figs. 2 and 6). As water begins to fill an empty Winnemucca
297 Lake, the basin essentially acts as a large evaporative pan. By the time lake level in Winnemucca
298 Lake reaches 1178 m, the lake has a surface area of about 250 km² and volume of 5.5 km³ (Fig.
299 6). The combined surface area of Pyramid at this same elevation and Winnemucca (~570 km²)
300 corresponds to an evaporative output of about 1 km³/yr, assuming an evaporation rate of 125
301 cm/yr (Milne, 1987). The magnitude of this output is significantly greater than the current mean
302 annual discharge into the basin of ~ 0.67 km³/yr.

303 The next higher sill in the Pyramid and Winnemucca basins is Emerson Pass, which
304 constrains spill from the north end of Pyramid Lake into the Smoke Creek Desert (Fig. 2). The
305 present elevation of this sill is about 1207 m but geologic mapping by Anderson et al. (2014)
306 indicates that Holocene alluvial fans shed from the Fox Range have buried Emerson Pass and
307 raised its elevation since the last time overflow occurred. Adams et al. (2008) suggested that the
308 functional overflow elevation of the sill was at about 1202 m based on the elevation of the crest
309 of a large barrier complex at the north end of Winnemucca Lake, whose size was attributed to a
310 stable lake level controlled by the sill. The actual elevation of Emerson Pass when spill was
311 occurring may have been 1-2 m below the crest of the barrier, however, accounting for wave run
312 up above still water level. Therefore, the elevation of Emerson Pass during periods of overflow
313 was probably closer to 1200 m.

314

315 **Geochronologic constraints**

316 Adams et al. (2008) presented several late Holocene radiocarbon ages for beach ridges between
317 1185 m and 1195 m at the north end of Winnemucca Lake, as well as a latest Pleistocene age for

318 the beach ridge at 1231 m. That data set is augmented with more radiocarbon ages from samples
319 collected from the trench through the 1231 m beach ridge and a group of luminescence ages
320 collected from the crests of beach ridges extending from 1177 m to 1231 m.

321 Figure 7 shows the stratigraphy and sedimentology of the 1231 m beach ridge and underlying
322 nearshore deposits with the locations and ages of dating samples plotted. These deposits are
323 primarily composed of discrete packages of basaltic gravel and sand separated from granitic sand
324 and grus units by angular unconformities and lags, and are numbered 1 through 8 in order of
325 decreasing relative age. The basalt sands and gravels were derived from the Lake Range to the
326 west of the trench and the granitic sands and gravels were derived from the Selenite Range to the
327 east (Fig. 2), although a few granitic clasts can be found in the basalt-dominated units and vice
328 versa. All of the units in this exposure are interpreted as wave-affected beach or nearshore
329 deposits, based on their relatively coarse nature and sedimentary features, but only units 7 and 8
330 represent the backsets of the 1231 m surface beach ridge.

331 The ages of seven radiocarbon samples and one tephra sample collected from various units
332 exposed in the trench demonstrate that this stack of primarily beach and nearshore deposits
333 accumulated between about 28,000 and 14,000 ^{14}C yr BP (Fig. 7) (Table 1), which represents a
334 time period when Lake Lahontan transgressed and regressed through this elevation range several
335 times (Benson et al., 2013a; Reheis et al., 2014). Two luminescence samples collected from the
336 backsets of the beach ridge (Unit 7) date to about 13.7 and 12 ka (Fig. 7 and Table 2), which are
337 younger than the radiocarbon samples collected from the same backsets. The two radiocarbon
338 ages from unit 7, however, are out of stratigraphic order with respect to the ages from units 2 – 6.

339 Additional luminescence samples were collected from beach ridges at 1218 m (11.1 ka and
340 57.2 ka), 1202 m (4.8 ka, 5.3 ka, 7.8 ka, 6.1 ka, and 6.9, ka), 1194 m (4.1 ka and 4.7 ka), 1190 m

341 (1.2 ka), 1185 m (0.05 ka and 0.02 ka), and 1177 m (0.22 ka and 0.34 ka) (Fig. 8; Table 2). The
342 IRSL ages for the 1194 m, 1185 m, and 1175 m ridges overlap at 1-sigma, whereas the five
343 sample ages for the 1202 m ridge and the two sample ages for the 1218 m ridge do not (Table 2).

344 A series of fluvial terraces are found along the distal reaches of the Truckee River, just
345 upstream from Pyramid Lake, which range in age from modern to about 12,700 ¹⁴C yr BP (Bell
346 et al., 2005a; Adams, 2012a). The youngest terraces are a few meters above the river channel and
347 the oldest are as much as 15 m above the channel. The Mazama tephra is found within fluvial
348 deposits, along with age-consistent radiocarbon samples, that are exposed in the lower parts of
349 the Nixon terrace (Q_{tn}) at an elevation just below 1200 m (Bell et al., 2005a), which indicates
350 that lake level was around or slightly below this elevation when the tephra was deposited (~7700
351 cal yr BP; Table 1). The elevations of the two radiocarbon samples from the Nixon terrace were
352 erroneously reported to be 1189 m by Adams et al. (2008). Based on a GPS survey and
353 elevations extracted from LiDAR data (Adams, 2012a), these elevations are herein corrected to
354 1198 m. The Mazama tephra and its slightly older sibling, the Tsoyawata tephra, are also found
355 ponded behind the 1202 m beach ridge at the north end of Winnemucca Lake (Adams et al.,
356 2008), which is consistent with a lake level around 1200 m.

357 The age and elevation of the downstream extent of the late Holocene fill-cut Q_{ty2} terrace of
358 Bell et al. (2005a) indicate that lake level was at about 1181 m around 500 cal yr BP (Table 1).
359 When the fill-cut Q_{ty3} terrace formed around 1240 cal yr BP (Bell et al., 2005a, b), it was graded
360 to a lake level at about 1183 m. Similarly, a fluvial gravel (Q_{try}) interbedded with lacustrine
361 deposits can be traced along the south wall of the deep trench cut by the Truckee River over the
362 last one hundred years to a point as low as about 1171 m, indicating that lake level was at least
363 that low at about 2100 cal yr BP (Bell et al., 2005a).

364 Several radiocarbon ages on human bones and associated cultural materials collected from
365 the northwest shore of Pyramid Lake constrain the timing of low lake levels during the late
366 Pleistocene and Holocene (Table 1) (Tuohy, 1988; Hattori and Tuohy, 1993; Edgar, 1997; Tuohy
367 and Dansie, 1997). In particular, low lake levels (~1154 m) are indicated at about 11,000 –
368 10,500, 6700, and 2500 cal yr BP. All of these samples were eroding out of beach or nearshore
369 deposits and only exposed when lake levels fell to artificially low levels in the mid-20th century
370 due to upstream water diversions.

371 Indirect data constraining the lake-level curve includes drowned trees in the nearshore zone
372 of Lake Tahoe that date from about 6400 to 4800 cal yr BP (Lindström, 1990). These trees
373 indicate extended periods in the middle Holocene when Lake Tahoe was below its natural rim.
374 By inference, flow down the Truckee River was likely greatly reduced, leading to relatively low
375 levels at Pyramid Lake (Benson et al., 2002).

376 The ages, elevations, and significance of all of the dating samples used to reconstruct the
377 post-Lahontan highstand lake-level curve of Pyramid and Winnemucca lakes are listed in Table
378 1 and plotted in figure 9. The part of the curve extending from about 16,000 – 7000 cal yr BP is
379 similar to the curve of Adams et al. (2008), but there is now more geochronologic data
380 constraining the curve from about 12,000 – 8000 cal yr BP. The middle to late Holocene part of
381 the curve is presented here for the first time.

382

383 **DISCUSSION**

384 The Pyramid-Winnemucca lake-level curve presented herein (Fig. 9) extends from the late
385 Pleistocene Lahontan highstand to the historical period and is constrained by multiple lines of
386 evidence employing a variety of dating techniques, in which samples were collected from a

387 range of depositional settings and landforms. Existing data was selected from the literature based
388 on the type of sample material and its context, particularly on whether the sample was deposited
389 above, at, or below lake level (Table 1). The principal dating technique was the radiocarbon
390 method, focusing on wood, charcoal, bones, and carbonate shells as sample material (Table 1).
391 These ages were augmented with a series of new IRSL ages on a suite of beach ridges at the
392 north end of Winnemucca Lake (Table 2 and Figs. 7 and 8).

393

394 **Sources of uncertainty**

395 The lake-level curve was drawn as a dotted line, constrained by the data points, but there could
396 have been, and likely were, significant fluctuations between some of these points that are not
397 captured in this curve. This uncertainty stems from a variety of sources that include analytical
398 errors as well as geological causes. Laboratory precision for the radiocarbon ages, which were
399 generated by many different researchers at many different labs, ranges from decadal to
400 centennial, with the larger errors typically associated with conventional ages that were generated
401 in the 1970s and 1980s (Table 1). When calibrated at 2-sigma, the errors expand to range from
402 about 100 years up to about 2500 years, depending on the original laboratory error as well as on
403 which part of the calibration curve the age falls.

404 Potential geological errors include radiocarbon samples that do not accurately reflect the age
405 of the sediments in which they were found and reservoir effects for samples that derived their
406 carbon from lake water. Both of these types of errors are difficult to assess but an attempt was
407 made to minimize their effects on the resultant lake-level curve by preferentially selecting from
408 the literature organic samples in known contexts that acquired their carbon from the atmosphere.
409 The reality of this kind of field research, however, dictates that one is often forced to sample

410 whatever carbon material that can be found in key landforms and outcrops, even if it is less than
411 ideal.

412 In many instances carbon material simply cannot be found, which is why IRSL dating was
413 utilized, but this technique also has its own set of associated uncertainties. At least two samples
414 were collected from each of the excavations on the seven different beach ridges (Table 2; Fig. 8).
415 Ideally, all samples from a single excavation would return the same age if all sand grains in the
416 deposit were last exposed to sunlight at the same time. For four of the seven beach ridges (1231
417 m, 1194 m, 1185 m, and 1175 m) this is indeed the case, where each of the pairs of ages overlap
418 at 1-sigma (Table 2). For the 1202 m ridge, however, the five samples collected from two
419 different excavations range from about 4.8 ka to 7.8 ka. The older age is preferred because of its
420 agreement with the ages of the Mazama and Tsoyawata tephra, which are ponded behind the
421 beach ridge (Fig. 8). For the 1218 m ridge, the age discrepancy is even larger with the two
422 sample ages of 11.1 ka and 57.2 ka collected just 12 cm apart.

423 Several processes may account for the age differences expressed by the duplicate samples.
424 The first may be incomplete bleaching of sand grains while a beach ridge is being formed, which
425 is consistent with the overprinted nature of nearshore environments (see below). The 57.1 ka age
426 from the 1218 m ridge may be explained by this process, as could the two ages from the
427 historical highstand (1177 m ridge), which appear to be as much as several hundred years too
428 old.

429 The second process may be eolian reworking of the lower, sandy beach ridges, which is
430 observed in the form of sand sheets, small dunes, and blowouts on these features, particularly at
431 their eastern ends (Fig. 8). Reworking of the beach sediment by eolian processes could
432 presumably lead to ages that were younger than the original beach sediment. This may be the

433 case with four of the samples from the 1202 m ridge and the samples from the 1185 m ridge
434 (Table 2).

435 A third source of geological uncertainty is in the often palimpsest record of near shore
436 environments, where wave action has the potential to rework sediment packages as lake level
437 rises and falls through a particular elevation range. This often leads to a complicated, reworked,
438 and overprinted sedimentary record in near shore environments that can span long periods of
439 time, and likely also contains significant unconformities. The trench excavated through the 1231
440 m beach ridge at Winnemucca Lake reveals a record that is probably typical of this type of
441 environment (Fig. 7). The ~2 m stack of lacustrine sediments exposed here represents an interval
442 of time lasting about 13,000 – 15,000 years during the late Pleistocene as Lake Lahontan
443 repeatedly rose and fell through this elevation range.

444 Adams et al. (2008) presented geomorphic and stratigraphic evidence that the 1231 m surface
445 ridge was formed after the Lahontan highstand and probably represented the maximum lake level
446 that occurred during the Younger Dryas period. At the time that the 2008 paper was written,
447 however, there was only a single radiocarbon age of $16,610 \pm 80$ ^{14}C yr BP that was generated
448 from shell fragments collected from the backsets of the surface beach ridge (Fig. 7). The shells
449 were interpreted as reworked material. An additional six radiocarbon samples collected from the
450 trench since 2008, as well as the presence of the Timber Lake tephra ($28,120 \pm 300$ ^{14}C yr BP;
451 Benson et al., 2003), suggests that the majority of these nearshore deposits (below unit 6, Fig. 7)
452 accumulated prior to the Lahontan highstand ($13,070 \pm 60$ ^{14}C yr BP; Adams and Wesnousky,
453 1998), although there are some slight age inversions in the upper part of the stratigraphy.

454 The two luminescence ages of about 12.7 and 13.1 ka generated from sediment samples
455 collected in the backsets of the 1231 m surface beach ridge suggest that this feature was formed

456 during the YD period (Fig. 7; unit 7), which is the same conclusion reached by Briggs et al.
457 (2005) and Adams et al. (2008). The older radiocarbon ages of about 15,500 and 16,600 ^{14}C yr
458 BP, collected from the same stratigraphic unit, highlights the potential difficulty of dating these
459 types of landforms and sediments in nearshore environments. In particular, abundant sediment,
460 along with shells, tufa fragments, and other dateable material, are likely reworked into younger
461 deposits each time a lake transgresses or regresses across a piedmont.

462 Some of the lower beach ridges at the north end of Winnemucca Lake also have radiocarbon
463 control that can be directly compared to the IRSL ages. The 1194 m beach ridge has a
464 radiocarbon age of 2720 – 2840 cal yr BP, while the luminescence age for this feature is 4.12 or
465 4.67 ka. Similarly, the radiocarbon age of the 1190 m beach ridge is 2860 – 3140 or 3250 – 3460
466 cal yr BP but the luminescence age is 1.17 ka. The disparity is even larger for the 1185 m beach
467 ridge, which has a radiocarbon age of 3780 – 4060 cal yr BP and a luminescence age of either
468 0.05 or 0.02 ka (Fig. 8; Tables 1 and 2). In short, none of the radiocarbon ages closely agrees
469 with the luminescence ages, which may also highlight the overprinted nature of beach deposits.
470 Therefore, caution is recommended when evaluating geochronologic data from these types of
471 settings. Based on the data included in this study, however, it is likely that there have been
472 multiple transgressions and regressions through the 1175-1195 m elevation range in the late
473 Holocene (Fig. 9).

474 The hypsometries of different basins and how they are connected may also highlight the
475 complex nature of these systems and increase the uncertainties when attempting to decipher their
476 histories. A good example of this is the nature and dynamics of the Mud Lake Slough sill that
477 connects the Pyramid and Winnemucca basins. A cursory examination of the channel where it
478 splits off from the Truckee River (Fig. 2) does not explain why historical lake levels in the two

479 subbasins of this system never achieved the same height even though the channel junction was
480 several times submerged by several meters. Only by looking many kilometers downstream is the
481 probable role of active sand dunes in blocking the channel revealed. If Pyramid Lake were to rise
482 today above the 1178.5 m elevation of the mouth of Mud Lake Slough, flow through the channel
483 would likely be blocked by the dunes until water seeped through or rose above the 1182 m height
484 of the obstruction, followed by quick incision through the pile of sand. When flow through Mud
485 Lake Slough ceased, the sand dune dam may also have reformed relatively quickly, judging by
486 the active nature of the dune complex (Fig. 5), enabled by a fresh supply of recently exposed
487 nearshore Pyramid Lake sand. The height of this periodic damming mechanism is likely to have
488 varied somewhat through time. The large (~28 km²) fan delta complex spread across the
489 southern bed of Winnemucca Lake (Fig. 2) may be the product of repeated formation and
490 destruction of the dune dam, moving the easily transportable sediment into the subbasin. This
491 apparent dynamism complicates efforts to date past lake levels in the 1175 – 1185 m range in
492 this system because the levels are not solely dependent on climate, but also on a suite of
493 geomorphic processes.

494

495 **Paleohydrologic implications**

496 This section compares the results of this study with previous studies and discusses the
497 implications of past lake-level fluctuations at Pyramid and Winnemucca lakes over the last
498 16,000 cal yr BP, but the emphasis is on the late Holocene part of the curve due to its relevance
499 for understanding possible magnitudes of future hydrologic changes. In particular, documenting
500 lake-level changes leads directly to quantifying absolute changes in water volume delivered by
501 the Truckee River drainage basin over centennial to millennial timescales.

502 The history of Pyramid and Winnemucca lakes has been studied by many different
503 researchers over the last 130 years, but probably the most relevant studies to compare to the
504 work presented herein are those of Benson et al. (1992, 2002, and 2013a, b) that focus on several
505 periods since the late Pleistocene. Benson et al. (1992) were the first to propose a Younger Dryas
506 highstand of about 1220 m at Pyramid Lake, but this interpretation is based on rock varnish
507 “ages” that are not thought to be reliable (e.g., Beck et al., 1998).

508 The study of Benson et al. (2013a) on tufa-covered petroglyphs at Winnemucca Lake covers
509 a similar time period to that of Adams et al. (2008) and the early part of the lake-level curve
510 presented herein (Fig. 9). Although there are some similarities in the lake-level curves, there are
511 also some significant differences. For example, the timing of the Lahontan highstand and
512 subsequent drop to low levels from 13,000 – 14,000 cal yr BP is similar for all reconstructions,
513 but the curves of Benson et al. (2013a, b) show a much lower lake level at this time than does the
514 curve from Adams et al. (2008) and the present curve. The present curve (Fig. 9) shows a distinct
515 rise to 1230 m at ~12,000 cal yr BP, during the Younger Dryas period, followed by a drop to
516 1154 m by 10,500 cal yr BP. This low lake level is constrained by the age and elevation of
517 sagebrush bark cordage found along the lake shore (Tuohy, 1988; Hattori and Tuohy, 1993), as
518 well as other data indicating low lake levels at this time (Fig. 9 and Table 1). In contrast, Benson
519 et al. (2013a) simply show a rise beginning at 13,000 cal yr BP to about 1210 m where lake level
520 remained until about 9800 cal yr BP. Benson et al. (2013b) drew this part of the curve slightly
521 higher, at about 1215 m and ended this highstand slightly sooner, at ~11,000 cal yr BP. These
522 parts of both Benson curves are based on the ages of tufa at elevations of about 1205 m, which
523 do not necessarily constrain how high the lake rose during this period.

524 Near the beginning of the middle Holocene, lake level was at about 1200 m when the
525 Tsoyawata and Mazama tephras were deposited (~7700 – 7900 cal yr BP; Bacon et al., 1983),
526 but fell to relatively low levels (~1154 m) by about 6800 cal yr BP (Fig. 9). This relatively large
527 lake-level change roughly corresponds to abrupt changes in the $\delta^{18}\text{O}$ record from a Pyramid Lake
528 core (Benson et al., 2002). The lake-level curve is queried for the next two thousand years
529 because there is no direct evidence of lake state. However, drowned tree stumps in Lake Tahoe
530 that date from about 6300 to 4800 cal yr BP (Lindström, 1990) provide indirect evidence for
531 reduced Truckee River input. The elevations, ages, and life spans of these stumps are interpreted
532 to indicate time periods when Lake Tahoe was below its natural rim and not contributing to the
533 Truckee River, which implies correspondingly low levels at Pyramid Lake (Benson et al., 2002).

534 Lake level began to rise again by ~5000 cal yr BP, reaching relatively high levels (>1178 –
535 1195 m) and remaining there until ~2800 cal yr BP, except for a brief drop to around 1174 m
536 around 3000 cal yr BP (Fig. 9). These shorelines represent the neopluvial period, which was first
537 defined by Allison (1982) based on relatively high late Holocene lake levels in the Summer Lake
538 basin of Oregon. The Summer Lake shorelines were not dated but Allison (1982) thought that
539 they were roughly 2000 to 4000 years old. Although the temporal range may vary slightly from
540 place to place, the spatial range of the neopluvial apparently extended from Oregon south
541 through Pyramid, Walker (Adams et al., 2014), Fallen Leaf (Noble et al., 2016), Mono (Stine,
542 1990), Owens (Bacon et al., 2018), Tulare (Negrini et al., 2006), and the Mojave (Enzel et al.,
543 2003) basins, all of which experienced high lake levels around 3500 to 4000 cal yr BP. This
544 signal also extended into the eastern Great Basin as cooler and wetter conditions are indicated by
545 the records at Ruby Marsh (Thompson, 1992) and the Great Salt Lake (Murchison, 1989;
546 Broughton et al., 2000; Broughton and Smith, 2016).

547 At Pyramid Lake, lake level reached its late Holocene highstand of about 1195 m at around
548 2800 cal yr BP, before dramatically falling to an elevation of about 1154 m by 2500 cal yr BP.
549 This large change in lake state (Fig. 9) is coincident with the start of the Late Holocene dry
550 period (Mensing et al., 2013), which was a multi-centennial long dry period affecting the Great
551 Basin from about 2800 to 1900 cal yr BP. This abrupt lake-level fall is constrained by the
552 presence of cultural materials found on the shore of Pyramid Lake by Tuohy (1988). Lake level
553 had recovered by about 1300 cal yr BP, reaching an elevation of about 1189 m.

554 During the subsequent Medieval Climate Anomaly and Little Ice Age, Pyramid levels
555 apparently fluctuated within a relatively narrow range from about 1172 to 1182 m (Fig. 9), or
556 essentially within the early historical range, prior to major Truckee River diversions (Hardman
557 and Venstrom, 1941). The $\delta^{18}\text{O}$ record of Benson et al. (2002) only fluctuates by about 1 per mil
558 during this period, also indicating low amplitude lake-level changes.

559 This relative stability is in contrast to the records of Walker Lake (Adams, 2007, 2018;
560 Hatchett et al., 2015), the Carson Sink (Adams, 2003, 2008), Mono Lake (Stine, 1990, 1994),
561 and Owens Lake (Bacon et al., 2018), all of which experienced relatively large lake-level
562 fluctuations over the last 1000 years or so. One potential explanation for this discrepancy is that
563 the Truckee drainage basin lies to the north of the drainage basins for Walker, Mono, and Owens
564 lakes. In tree-ring based maps showing the spatio-temporal distributions of the Medieval
565 droughts in western North America (Cook et al., 2010), the Truckee basin is just to the north of
566 the areas that were most severely affected by these droughts and therefore may have escaped
567 their worst effects. Similarly, the Medieval pluvial (875 – 829 cal yr BP; Cook et al., 2010) did
568 not seem to have much of an effect in the Pyramid basin, even though an unusually large lake
569 was present at this time in the Carson Sink to the east (Adams, 2003, 2008, 2012b, 2018).

570 Documented lake-level changes were converted into other metrics to provide additional
571 insight into the magnitude of hydrologic changes over the late Holocene. Figure 10 presents
572 three derivative lake-state curves that were constructed using the hypsometric relations of the
573 basin (Fig. 6) and are expressed in terms of surface area changes, evaporation volume changes,
574 and lake volume changes through time. Combining these metrics with knowledge of Truckee
575 River discharge and historical lake evaporation rates provides a more complete view of the
576 magnitude of hydrologic changes that have occurred in this system over the last 5000 years.

577 During the late Holocene, lake levels at Pyramid and Winnemucca lakes have fluctuated by
578 about 40 meters, which corresponds to changes in lake-surface area ranging from about 450 to
579 900 km², or about a factor of two (Fig. 10). Assuming an annual lake-surface evaporation rate
580 around 125 to 135 cm/yr (Milne, 1987), the range in the total annual volume of water evaporated
581 from Pyramid and Winnemucca lakes has ranged from about 0.45 to 0.95 km³, also roughly a
582 factor of two. Similarly, the volume of these lakes has fluctuated by about a factor of two over
583 the late Holocene, ranging from about 25 to 55 km³ (Fig. 10). The surface area and volume
584 constraints imposed by the hypsometries of the basins (Fig. 6) therefore indicates that discharge
585 must have been significantly higher than the modern average (~0.67 km³), for a period of years
586 or decades, in order for lake levels to have risen above 1178 – 1182 m and achieve the late
587 Holocene highstands (Fig. 9).

588 The largest drop in Pyramid and Winnemucca lake levels occurred around 2800 cal yr BP
589 when surface elevation fell from 1195 m to about 1154 m, and the lake basin lost approximately
590 30 km³ of water (Figs. 9 and 10). The radiocarbon data do not provide much precision in
591 constraining the rate of lake-level fall, but based on modern evaporation rates this change must
592 have occurred over at least several to many decades.

593 The historical drop from about 1180 m in 1910 to Pyramid's historical lowstand of about
594 1154 m in 1967 (Fig. 4) may provide a similar but modern example of how much inflow had to
595 be decreased to cause a 26 m drop and loss of about 20 km³ of water in about six decades. Figure
596 3 shows the annual discharge flowing past two gages along the Truckee River, one above where
597 the largest withdrawals occur (Farad) and one below where they occur (Below Derby). Even
598 though in large flow years, the annual totals are similar, during most years about one half of the
599 Truckee River annual flow is diverted for other uses, which has caused the precipitous drop in
600 Pyramid levels over the last century. Suffice it to say that a 50% reduction in natural flow from
601 the Truckee River drainage occurring over several decades would present a serious water supply
602 issue in this region. Based on the late Holocene record of Pyramid Lake, however, this
603 magnitude of drought is within the realm of possibility for future climatic scenarios, even
604 without considering the potentially compounding effects of climate change.

605 Overall, the late Holocene lake-level fluctuations at Pyramid and Winnemucca lakes offer a
606 perspective on the magnitude and duration of climate extremes possible in the northern Sierra
607 Nevada, both on the dry and wet ends of the climatic continuum. This is because the climate
608 boundary conditions that govern eastern Pacific Ocean-western North America climate have
609 been in place for about the last 5000 years (e.g., Wanner et al., 2008), so whatever has occurred
610 over the last few thousand years may again be possible in the future. Thus, understanding the late
611 Holocene paleohydrology of a region helps define possible future hydrologic variability.

612

613 **CONCLUSIONS**

614 A new lake-level curve is presented for the Pyramid and Winnemucca lake basins in western
615 Nevada that spans the time period from when Lake Lahontan occupied the basins and was

616 carving shorelines at an elevation of about 1338 m through to the present when Pyramid Lake
617 would naturally fluctuate around 1175 – 1182 m. This curve is based on existing radiocarbon
618 data culled from the literature, new radiocarbon ages, and new luminescence ages collected from
619 beach ridges at the north end of the Winnemucca Lake basin.

620 Since the late Pleistocene highstand of Lake Lahontan, lake-level fluctuations have been
621 decreasing in amplitude through time. The Younger Dryas highstand in Pyramid and
622 Winnemucca lakes is confirmed to have reached an elevation of about 1230 m; this highstand
623 also integrated a number of other subbasins in the western part of the Lahontan system (Adams
624 et al., 2008). During the Holocene, however, lake levels have alternated between lows of about
625 1154 m to a highstand at about 1200 m that was roughly coincident with the eruption of the
626 Mazama tephra at about 7700 cal yr BP. After relatively low levels in the middle Holocene, the
627 lake again expanded to reach levels around 1185 – 1190 m during the neopluvial period (~4800 –
628 3400 cal yr BP) before crashing to low levels during the late Holocene dry period. By about 2000
629 cal yr BP, lake levels had recovered, briefly rising to about 1189 m by about 1200 cal yr BP.
630 Since that time, lake levels have fluctuated within a relatively narrow elevation range of about
631 1170 – 1180 m, except for the historical period when they have been artificially lowered due to
632 upstream water diversions.

633 These late Holocene lake-surface elevation changes correspond to surface area changes
634 ranging from about 500 – 900 km² and volumetric changes ranging from about 25 – 55 km³.
635 Based on modern Truckee River inflow records and Pyramid Lake evaporation rates, these
636 changes must have occurred over at least decades, suggesting that droughts that have occurred in
637 this drainage basin have been far more severe than any droughts that have occurred during the
638 historical period.

639 Accurately defining the timing, magnitude, and duration of late Holocene lake-level
640 fluctuations is relevant to water supply concerns because these changes have occurred under
641 approximately the same climate boundary conditions that exist today. Any climate-induced
642 hydrologic fluctuations that have occurred in these basins over the last few thousand years are
643 still possible in the future. Another way of thinking about this is that defining the magnitude of
644 lake-level changes during the late Holocene places bounds on possible future fluctuations in
645 water supply.

646

647 **ACKNOWLEDGEMENTS**

648 This work was partially funded by National Science Foundation grant EAR1252225 and by the
649 General Frederick Lander Endowment administered by the Desert Research Institute, but the
650 authors are responsible for all analyses and interpretations. We thank Mike Lawson and Chris
651 McGuire for their help in luminescence sample collection, Wendy Barrera and Tom Capaldi for
652 sample preparation, and Nathan Brown for sample preparation and measurements. Adams thanks
653 John Bell for the many helpful discussions and field trips to the lower Truckee River over the
654 years and Wally Broecker for the multiple radiocarbon ages from the 1231 m trench at
655 Winnemucca Lake. Sophie Baker was very helpful in preparing some of the figures in this paper.
656 Helpful reviews by Marith Reheis, David Miller, Jim O’Conner, and Noah Abramson improved
657 the clarity and content of this manuscript.

658

659 **REFERENCES**

660 Adams, K.D., 2003, Age and paleoclimatic significance of late Holocene lakes in the Carson
661 Sink, NV, USA: Quaternary Research, v. 60, p. 294-306.

662 Adams, K.D., 2007, Late Holocene sedimentary environments and lake-level fluctuations at
663 Walker Lake, Nevada, USA: Geological Society of America Bulletin, v. 119, p. 126-139.

664 Adams, K.D., 2008, Lake-level fluctuations in the western Great Basin during the Medieval
665 Climate Anomaly: episodes of both drier and wetter periods than modern: Geological
666 Society of America Abstracts with Programs, v. 40, p. 227.

667 Adams, K.D., 2010, Lake levels and sedimentary environments during deposition of the Trego
668 Hot Springs and Wono tephras in the Lake Lahontan basin, Nevada, USA: Quaternary
669 Research, v. 73, p. 118-129.

670 Adams, K.D., 2012a, Response of the Truckee River to lowering base level at Pyramid Lake,
671 Nevada, based on historical air photos and LiDAR data: Geosphere, v. 8, p. 607-627.

672 Adams, K.D., 2012b, Late Holocene paleohydrology of the western Great Basin, American
673 Quaternary Association, 22nd Biennial Meeting, Program and Abstracts: Duluth, MN, p.
674 8.

675 Adams, K.D., 2018, Late Holocene paleohydrology of Walker Lake and the Carson Sink in the
676 western Great Basin, Nevada, USA: Quaternary Science Reviews, in review.

677 Adams, K.D., and Wesnousky, S.G., 1998, Shoreline processes and the age of the Lake Lahontan
678 highstand in the Jessup embayment, Nevada: Geological Society of America Bulletin, v.
679 110, p. 1318-1332.

680 Adams, K.D., Goebel, T., Graf, K., Smith, G.M., Camp, A.J., Briggs, R.W., and Rhode, D.,
681 2008, Late Pleistocene and early Holocene lake-level fluctuations in the Lahontan basin,
682 Nevada: Implications for the distribution of archaeological sites: Geoarchaeology: An
683 International Journal, v. 23, p. 608-643.

684 Adams, K.D., Bacon, S.N., Lancaster, N., Rhodes, E.J., and Negrini, R.M., 2014, How wet can it
685 get? Defining future climate extremes based on late Holocene lake-level records:
686 Geological Society of America Abstracts with Programs, v. 46, p. 745.

687 Allison, I.S., 1982, Geology of pluvial Lake Chewaucan, Lake County, Oregon: Corvallis, OR,
688 Oregon State University Press, 79 p.

689 Anderson, R.F., Faulds, J.E., and Dering, G.M., 2014, Preliminary geologic map of the central
690 Lake Range, southern Fox Range, and northern Terraced Hills, Emerson Pass Geothermal
691 Area, Washoe County, Nevada: Reno, Nevada Bureau of Mines and Geology Open-File
692 Report 13-10, 1:24,000 scale.

693 Atwood, G., 1994, Geomorphology applied to flooding problems of closed-basin lakes -
694 Specifically Great-Salt-Lake, Utah: Geomorphology, v. 10, p. 197-219.

695 Bacon, C.R., 1983, Eruptive history of Mount Mazama and Crater Lake Caldera, Cascade Range,
696 U.S.A.: Journal of Volcanology and Geothermal Research, v. 18, p. 57-115.

697 Bacon, S.N., Lancaster, N., Stine, S., Rhodes, E.J., McCarley Holder, 2018, A continuous 4000-
698 year lake-level record of Owens Lake, south-central Sierra Nevada, California, USA:
699 Quaternary Research, p. 1-27, doi:10.1017/qua.2018.50.

700 Beck, W., Donahue, D.J., Jull, A.J.T., Burr, G., Broecker, W.S., Bonani, G., Hajdas, I., and
701 Malotki, E., 1998, Ambiguities in direct dating of rock surfaces using radiocarbon
702 measurements: Science, v. 280, 5372, p. 2132-2139.

703 Bell, J.W., House, P.K., and Briggs, R.W., 2005a, Geologic map of the Nixon area, Washoe
704 County, Nevada: Reno, Nevada, Nevada Bureau of Mines and Geology Map 152.

705 Bell, J.W., Garside, L.J., and House, P.K., 2005b, Geologic Map of the Wadsworth quadrangle,
706 Washoe County, Nevada: Reno, Nevada, Nevada Bureau of Mines and Geology Map
707 153.

708 Benson, L.V., 1978, Fluctuations in the level of pluvial Lake Lahontan during the last 40,000
709 years: *Quaternary Research*, v. 9, p. 300-318.

710 Benson, L.V., and Thompson, R.S., 1987, The physical record of lakes in the Great Basin, *in*
711 Ruddiman, W.F., and Wright, H.E., Jr., eds., *North America and adjacent oceans during*
712 *the last deglaciation*: Boulder, CO, United States, Geological Society of America, p. 241-
713 260.

714 Benson, L.V., Currey, D.R., Dorn, R.I., Lajoie, K.R., Oviatt, C.G., Robinson, S.W., Smith, G.I.,
715 and Stine, S., 1990, Chronology of expansion and contraction of four Great Basin lake
716 systems during the past 35,000 years: *Palaeogeography, Palaeoclimatology,*
717 *Palaeoecology*, v. 78, p. 241-286.

718 Benson, L.V., Currey, D.R., Lao, Y., and Hostetler, S.W., 1992, Lake-size variations in the
719 Lahontan and Bonneville basins between 13,000 and 9000 ¹⁴C yr BP: *Palaeogeography,*
720 *Palaeoclimatology, Palaeoecology*, v. 95, p. 19-32.

721 Benson, L., Kashgarian, M., and Rubin, M., 1995, Carbonate deposition, Pyramid Lake subbasin,
722 Nevada; 2, Lake levels and polar jet stream positions reconstructed from radiocarbon
723 ages and elevations of carbonates (tufas) deposited in the Lahontan Basin:
724 *Palaeogeography, Palaeoclimatology, Palaeoecology*, v. 117, p. 1-30.

725 Benson, L., Kashgarian, M., Rye, R., Lund, S., Paillet, F., Smoot, J., Kester, C., Mensing, S.,
726 Meko, D., and Lindstrom, S., 2002, Holocene multidecadal and multicentennial droughts

727 affecting northern California and Nevada: *Quaternary Science Reviews*, v. 21, p. 659-
728 682.

729 Benson, L., Liddicoat, J., Smoot, J., Sarna-Wojcicki, A., Negrini, R., and Lund, S., 2003, Age of
730 the Mono Lake excursion and associated tephra: *Quaternary Science Reviews*, v. 22, p.
731 135-140.

732 Benson, L.V., Hattori, E.M., Southon, J., and Aleck, B., 2013a, Dating North America's oldest
733 petroglyphs, Winnemucca Lake subbasin, Nevada: *Journal of Archaeological Science*, v.
734 40, p. 4466-4476.

735 Benson, L.V., Smoot, J.P., Lund, S.P., Mensing, S.A., Foit Jr., F.F., and Rye, R.O., 2013b,
736 Insights from a synthesis of old and new climate-proxy data from the Pyramid and
737 Winnemucca lake basins for the period 48 to 11.5 cal ka: *Quaternary International*, v.
738 310, p. 62-82.

739 Bonham, H.F., and Papke, K.G., 1969, Geology and mineral resources of Washoe and Storey
740 counties, Nevada, with a section on industrial rock and mineral deposits, Nevada Bureau
741 of Mines and Geology Bulletin 70.

742 Born, S.M., 1972, Late Quaternary history, deltaic sedimentation, and mudlump formation at
743 Pyramid Lake, Nevada: Reno, Nevada, Center for Water Resources, Desert Research
744 Institute, 97 p.

745 Briggs, R.W., Wesnousky, S.G., and Adams, K.D., 2005, Late Pleistocene and late Holocene
746 lake highstands in the Pyramid Lake subbasin of Lake Lahontan, Nevada, USA:
747 *Quaternary Research*, v. 64, p. 257-263.

748 Broecker, W.S., and Orr, P.C., 1958, Radiocarbon chronology of Lake Lahontan and Lake
749 Bonneville: *Geological Society of America Bulletin*, v. 69, p. 1009-1032.

750 Broecker, W.S., and Kaufman, A., 1965, Radiocarbon chronology of Lake Lahontan and Lake
751 Bonneville; Part 2, Great Basin: Geological Society of America Bulletin, v. 76, p. 537-
752 566.

753 Broecker, W.S., McGee, D., Adams, K.D., Cheng, H., Edwards, L., Oviatt, C.G., and Quade, J.,
754 2009, A Great Basin-wide dry episode during the first half of the Mystery Interval?:
755 Quaternary Science Reviews, v. 28, p. 2557-2563.

756 Broughton, J.M., Madsen, D.B., and Quade, J., 2000, Fish remains from Homestead Cave and
757 lake levels of the past 13,000 years in the Bonneville Basin: Quaternary Research, v. 53,
758 p. 392-401.

759 Broughton, J.M., and Smith, G.R., 2016, The fishes of Lake Bonneville: Implications for
760 drainage history, biogeography, and lake levels, in Oviatt, C.G., and Shroder, J.F., eds., Lake
761 Bonneville: A Scientific update: Elsevier, Developments in Earth Surface Processes, v. 20,
762 Amsterdam, Netherlands, p. 292-351.

763 Cook, E.R., Seager, R., Heim, R.R.J., Vose, R.S., Herweijer, C., and Woodhouse, C., 2010,
764 Megadroughts in North America: placing IPCC projections of hydroclimatic change in a
765 long-term palaeoclimate context: Journal of Quaternary Science, v. 25, p. 48-61.

766 Daly, C., Halbleib, M., Smith, J., Gibson, W.P., Doggett, M.K., and Taylor, G.H., 2008,
767 Physiographically sensitive mapping of climatological temperature and precipitation
768 across the conterminous United States: International Journal of Climatology, v. 28, p.
769 2031-2064.

770 Dansie, A.J., and Jerrems, W.J., 2005, More bits and pieces: A new look at Lahontan chronology
771 and human occupation. In R. Bonnicksen, B.T. Lepper, D. Stanford, & M.R. Waters
772 (Eds.), Paleoamerican origins: Beyond Clovis: College Station, Center for the Study of
773 the First Americans, Texas A&M University, p. 51-73.

774 Edgar, H.J.H., 1997, Paleopathology of the Wizards Beach Man (AHUR 2023) and the Spirit
775 Cave mummy (AHUR 2064): Nevada Historical Society Quarterly, v. 40, p. 57-61.

776 Eisses, A.K., Kell, A., Kent, G.M., Driscoll, N.W., Baskin, R.L., Smith, K.D., Karlin, R.E.,
777 Louie, J.N., and Pullammanappallil, S.K., 2015, New constraints on fault architecture,
778 slip rates, and strain partitioning beneath Pyramid Lake, Nevada: Geosphere, v. 11, no. 3,
779 22 p.

780 Enzel, Y., Wells, S.G., and Lancaster, N., 2003, Late Pleistocene lakes along the Mojave River,
781 southeast California, *in* Enzel, Y., Wells, S.G., and Lancaster, N., eds.,
782 Paleoenvironments and paleohydrology of the Mojave and southern Great Basin deserts:
783 Boulder, Geological Society of America Special Paper 368, p. 61-77.

784 Harding, S.T., 1965, Recent variations in the water supply of the western Great Basin: Berkeley,
785 California, Water Resources Center Archives, University of California, 225 p.

786 Hardman, G., and Venstrom, C., 1941, A 100-year record of Truckee River runoff estimated
787 from changes in levels and volumes of Pyramid and Winnemucca lakes: Transactions of
788 the American Geophysical Union, p. 71-90.

789 Hatchett, B. J., D. P. Boyle, A. E. Putnam, and Bassett, S.D., 2015, Placing the 2012–2015
790 California-Nevada drought into a paleoclimatic context: Insights from Walker Lake,
791 California-Nevada, USA: Geophysical Research Letters, v. 42, p. 8632–8640,
792 doi:[10.1002/2015GL065841](https://doi.org/10.1002/2015GL065841).

793 Hattori, E.M., 1982, The archeology of Falcon Hill, Winnemucca Lake, Washoe County,
794 Nevada: Carson City, NV, Nevada State Museum Anthropological Papers Number 18.

795 Hattori, E.M., and Tuohy, D.R., 1993, Prehistoric human occupation and changing lake levels at
796 Pyramid and Winnemucca lakes, Nevada, Proceedings of the workshop "Ongoing

797 paleoclimatic studies in the northern Great Basin": Reno, NV, U.S. Geological Survey
798 Circular 1119, p. 31-34.

799 Horton, G.A., 1997, Truckee River chronology: A chronological history of Lake Tahoe and the
800 Truckee River and related water issues, Nevada Water Basin Information and
801 Chronology Series: Carson City, Nevada, Nevada Division of Water Planning,
802 Department of Conservation and Natural Resources, 216 p.

803 Houghton, J.G., Sakamoto, C.M., and Gifford, R.O., 1975, Nevada's weather and climate: Reno,
804 Nevada Bureau of Mines and Geology, Special Publication 2, 78 p.

805 Lindström, S., 1990, Submerged tree stumps as indicators of mid-Holocene aridity in the Lake
806 Tahoe region: *Journal of California and Great Basin Anthropology*, v. 12, p. 146-157.

807 Mensing, S.A., Sharpe, S.E., Tunno, I., Sada, D.W., Thomas, J.M., Starratt, S., and Smith, J.,
808 2013, The late Holocene Dry Period: multiproxy evidence for an extended drought
809 between 2800 and 1850 cal yr BP across the central Great Basin, USA: *Quaternary
810 Science Reviews*, v. 78, p. 266-282.

811 Milne, W., 1987, A comparison of reconstructed lake-level records since the mid-1880s of some
812 Great Basin lakes [M.S. thesis]: Golden, Colorado School of Mines.

813 Morrison, R.B., 1991, Quaternary stratigraphic, hydrologic, and climatic history of the Great
814 Basin, with emphasis on Lake Lahontan, Bonneville, and Tecopa, *in* Morrison, R.B., ed.,
815 Quaternary nonglacial geology; conterminous U.S.: Boulder, CO, United States,
816 Geological Society of America, p. 283-320.

817 Murchison, S.B., 1989, Fluctuation history of Great Salt Lake, Utah, during the last 13,000 years
818 [Ph.D. Dissertation thesis]: Salt Lake City, UT, University of Utah.

819 Negrini, R.M., 2002, Pluvial Lake Sizes in the Northwestern Great Basin throughout the
820 Quaternary Period, *in* Hershler, R., Madsen, D.B., and Currey, D., eds., Great Basin
821 Aquatic Systems History: Smithsonian Contributions to the Earth Sciences, Volume 33:
822 Washington, D.C., Smithsonian Institution Press, p. 11-52.

823 Negrini, R.M., Wigand, P.E., Draucker, S., Gobalet, K., Gardner, J.K., Sutton, M.Q., and Yohe,
824 R.M., 2006, The Rambla highstand shoreline and the Holocene lake-level history of
825 Tulare Lake, California, USA: Quaternary Science Reviews, v. 25, p. 1599-1618.

826 Noble, P.J., Ball, G.I., Zimmerman, S.H., Maloney, J., Smith, S.B., Kent, G., Adams, K.D.,
827 Karlin, R.E., and Driscoll, N., 2016, Holocene paleoclimate history of Fallen Leaf Lake,
828 CA., from geochemistry and sedimentology of well-dated sediment cores: Quaternary
829 Science Reviews, v. 131, p. 193-210.

830 Prokopovich, N.P., 1983, Alteration of alluvium by natural gas in the Pyramid Lake area,
831 Nevada: Bulletin of the Association of Engineering Geologists, v. 20, p. 185-196.

832 Reheis, M.C., Adams, K.D., Oviatt, C.G., and Bacon, S.N., 2014, Pluvial lakes in the Great
833 Basin of the western United States: A view from the outcrop: Quaternary Science
834 Reviews, v. 97, p. 33-57.

835 Reimer, P.J., Bard, E., Bayliss, A., Beck, J.W., Blackwell, P.G., Bronk Ramsey, C., Buck, C.E.,
836 Cheng, H., Edwards, R.L., Friedrich, M., Grootes, P.M., Guilderson, T.P., Haflidason, H.,
837 Hajdas, I., Hatté, C., Heaton, T.J., Hogg, A.G., Hughen, K.A., Kaiser, K.F., Kromer, B.,
838 Manning, S.W., Niu, M., Reimer, R.W., Richards, D.A., Scott, E.M., Southon, J.R.,
839 Turney, C.S.M., van der Plicht, J., 2013, IntCal13 and MARINE13 radiocarbon age
840 calibration curves 0-50000 years cal BP: Radiocarbon, v. 55, no.4, p. 1869-1887, doi:
841 10.2458/azu_js_rc.55.16947.

842 Rhodes, E.J., 2015, Dating sediments using potassium feldspar single grain IRSL: Initial
843 methodological considerations: *Quaternary International*, v. 362, p. 14-22.

844 Russell, I.C., 1885, Geological history of Lake Lahontan, a Quaternary lake in northwestern
845 Nevada, U.S. Geological Survey Monograph 11, 288 p.

846 Sigl, M., Fudge, T.J., Winstrup, M., Cole-Dai, J., Ferris, D., McConnell, J.R., Taylor, K.C.,
847 Welton, K.C., Woodruff, T.E., Adolphi, F., Bisiaux, M., Brook, E.J., Buizert, C., Caffee,
848 M.W., Dunbar, N.W., Edwards, R., Geng, L., Iverson, N., Koffman, B., Layman, L.,
849 Maselli, O.J., McGwire, K., Muscheler, R., Nishiizumi, K., Pasteris, D.R., Rhodes, R.H.,
850 and Sowers, T.A., 2016, The WAIS Divide deep ice core WD2014 chronology - Part 2:
851 Annual-layer counting (0-31 ka BP): *Climate of the Past*, v. 12, p. 769-786.

852 Smith, G.I., and Street-Perrott, F.A., 1983, Pluvial lakes of the Western United States, *in* Porter,
853 S.C., ed., *The late Pleistocene.*: Minneapolis, MN, United States, Univ. Minn. Press, p.
854 190-212.

855 Stewart, J. H., 1978, Basin and Range structure in western North America, A review, *in* Smith,
856 R. B., and Eaton, G. P., eds., *Cenozoic tectonics and regional geophysics of the Western*
857 *Cordillera: Geological Society of America Memoir 152*, p. 1–32.

858 Stewart, J. H., 1988, Tectonics of the Walker Lane belt, western Great Basin: Mesozoic and
859 Cenozoic deformation in a zone of shear, *in* Ernst, W. G., ed., *Metamorphism and cause*
860 *of evolution of the western United States: Ruby Volume 7: Englewood Cliffs, New*
861 *Jersey, Prentice-Hall*, p. 683–713.

862 Stine, S., 1990, Late Holocene fluctuations of Mono Lake, California: *Palaeogeography,*
863 *Palaeoclimatology, Palaeoecology*, v. 78, p. 333-381.

864 Stine, S., 1994, Extreme and persistent drought in California and Patagonia during mediaeval
865 time: *Nature*, v. 369, p. 546-549.

866 Thompson, R.S., 1992, Late Quaternary environments in Ruby Valley, Nevada: *Quaternary*
867 *Research*, v. 37, p. 1-15.

868 Thompson, R.S., Benson, L., and Hattori, E.M., 1986, A revised chronology for the last
869 Pleistocene lake cycle in the central Lahontan basin: *Quaternary Research*, v. 25, p. 1-9.

870 Tuohy, D.R., 1988, Artifacts from the northwestern Pyramid Lake shoreline, *in* Willig, J.A.,
871 Aikens, C.M., and Fagan, J.L., eds., Early human occupation in far western North
872 America: the Clovis-Archaic interface: Carson City, Nevada State Museum
873 Anthropological Papers Number 21, p. 201-216.

874 Tuohy, D.R., and Dansie, A.J., 1997, New information regarding early Holocene manifestations
875 in the western Great Basin: *Nevada Historical Society Quarterly*, v. 40, p. 24-53.

876 Unruh, J., Humphrey, J., and Barron, A., 2003, Transtensional model for the Sierra Nevada
877 frontal fault system, eastern California: *Geology*, v. 31, p. 327-330.

878 Van Buer, N., 2012, Preliminary geologic map of the Sahwave and Nightingale Ranges,
879 Churchill, Pershing, and Washoe counties, Nevada: Nevada Bureau of Mines and
880 Geology Open File 12-2, 1:62,500 scale, 12 p.

881 Walker, M.J.C., Berkelhammer, M., Bjorck, S., Cwynar, L.C., Fisher, D.A., Long, A.J., Lowe,
882 J.J., Newnham, R.M., Rasmussen, S.O., and Weiss, H., 2012, Formal subdivision of the
883 Holocene series/epoch: a discussion paper by a working group of INTIMATE
884 (Integration of ice-core, marine and terrestrial records) and the Subcommittee on
885 Quaternary Stratigraphy (International Commission on Stratigraphy): *Journal of*
886 *Quaternary Science*, v. 27, p. 649-659.

887 Wanner, H., Beer, J., Butikofer, J., Crowley, T.J., Cubasch, U., Fluckiger, J., Goosse, H.,
888 Gosjean, M., Joos, F., Kaplan, J., Kuttel, M., Muller, S., Prentice, I.C., Solomina, O.,
889 Stocker, T.F., Tarasov, P., Wagner, M., and Widmann, M., 2008, Mid- to Late Holocene
890 climate change: an overview: *Quaternary Science Reviews*, v. 27, p. 1791-1828.
891 Wesnousky, S.G., 2005, Active faulting in the Walker Lane: *Tectonics*, v. 24, TC3009,
892 doi:10.1029/2004TC001645.
893
894

895 **FIGURE CAPTIONS**

896 Figure 1. Overview map of the Truckee River drainage basin (thin white line) showing the
897 locations of Pyramid (PL) and Winnemucca (WL) lakes in the lower basin and Lake Tahoe (T)
898 near the headwaters. HL = Honey Lake, SCBR = Smoke Creek-Black Rock Desert, F = Farad
899 gage, BD = Below Derby gage. The background is mean annual PRISM precipitation (MAP)
900 (Daly et al., 2008). The inset map shows the location of the Truckee River basin with respect to
901 the western U.S. For the full explanation of color symbols, see the online version.

902
903 Figure 2. Overview map of the Pyramid and Winnemucca lake basins showing the distribution of
904 geographic features mentioned in the text. Pyramid Lake is shown at the 1160 m level with
905 hillshaded bathymetry after Eisses et al. (2015). The thin white line shows the extent of the
906 historic highstands at Pyramid (1182 m) and Winnemucca (1175 m) lakes and the thin black line
907 shows the extent of the integrated lake basins when they were at an elevation of 1200 m. The
908 thin yellow line shows the extent of the fan delta emanating from the north end of Mud Lake
909 Slough. Locations of figures 5 and 8 are also shown. For the full explanation of color symbols,
910 see the online version.

911
912 Figure 3. Annual discharge volumes for two points along the Truckee River. The Farad gage
913 record represents discharge in the upper part of the basin, upstream of the largest withdrawals,
914 and the Below Derby gage record represents discharge that actually reaches Pyramid Lake.
915 Locations of gages are shown in figure 1.

916

917 Figure 4. Historical lake-level changes at Pyramid and Winnemucca lakes from the mid-19th
918 century to the present. Data from Hardman and Venstrom (1941) and the USGS
919 (https://waterdata.usgs.gov/nv/nwis/inventory/?site_no=10336500&agency_cd=USGS). Derby
920 Dam, where about 50% of the mean annual discharge of the Truckee River is diverted, was
921 installed in 1906.

922

923 Figure 5. Aerial image of the active dune field (location on Fig. 2) that is blocking the Mud Lake
924 Slough channel. Flow in the channel is from south to north. The green line represents the 1183 m
925 contour on the Pyramid Lake side of the dune barrier. For the full explanation of color symbols,
926 see the online version.

927

928 Figure 6. Hypsometric relations between lake-surface elevation, lake-surface area, and lake
929 volume for Pyramid and Winnemucca lakes. The flat parts of the curves represent Pyramid Lake
930 spilling at an elevation of 1183 m and filling Winnemucca Lake. For the full explanation of color
931 symbols, see the online version.

932

933 Figure 7. Log of the west wall of the trench through the 1231 m beach ridge at the north end of
934 Winnemucca Lake showing the arrangement of stratigraphic units and the distribution of dating
935 samples. The location of this trench is shown in figure 8. The age of the Timber Lake tephra is
936 from Benson et al. (2003).

937

938 Figure 8. Map of beach ridges at the north end of Winnemucca Lake showing the locations and
939 results of dating samples. Yellow circles are radiocarbon samples, green circles are luminescence

940 samples, and the red star indicates the locations of the Mazama and Tsoyawata tephras. Thin
941 black lines delineate beach ridge crests and the elevations of several of the crests are labeled. See
942 figure 2 for location.

943

944 Figure 9. Lake-level curve for the Pyramid and Winnemucca lake basins extending from the late
945 Pleistocene highstand of Lake Lahontan to the present. The main subdivisions of the late
946 Pleistocene and Holocene along the bottom of the graph are from Broecker et al. (2009), Walker
947 et al. (2012), and Sigl et al. (2016) and are as follows: BD = Big Dry, BW = Big Wet, BA =
948 Bølling-Allerød, YD = Younger Dryas, EH = Early Holocene, MH = Middle Holocene, and LH
949 = Late Holocene. Further subdivision of the middle and late Holocene include, LTT = the time
950 period over which trees were growing on the shore of Lake Tahoe below its natural rim
951 (Lindström, 1990), NP = Neopluvial (Allison, 1982), LHDP = Late Holocene dry period
952 (Mensing et al., 2013), MCA = Medieval Climate Anomaly (Stine, 1994; Cook et al., 2010), LIA
953 = Little Ice Age (Cook et al., 2010), and H = Historical period. For the full explanation of color
954 symbols, see the online version.

955

956 Figure 10. Plots of fluctuations in lake state over the last 5000 years. A) Simplified lake-surface
957 elevation changes. B) Fluctuations in surface area (solid line) and total annual evaporation
958 (dashed line), which is based on surface area. C) Changes in lake volume over time.

959

Figure 1

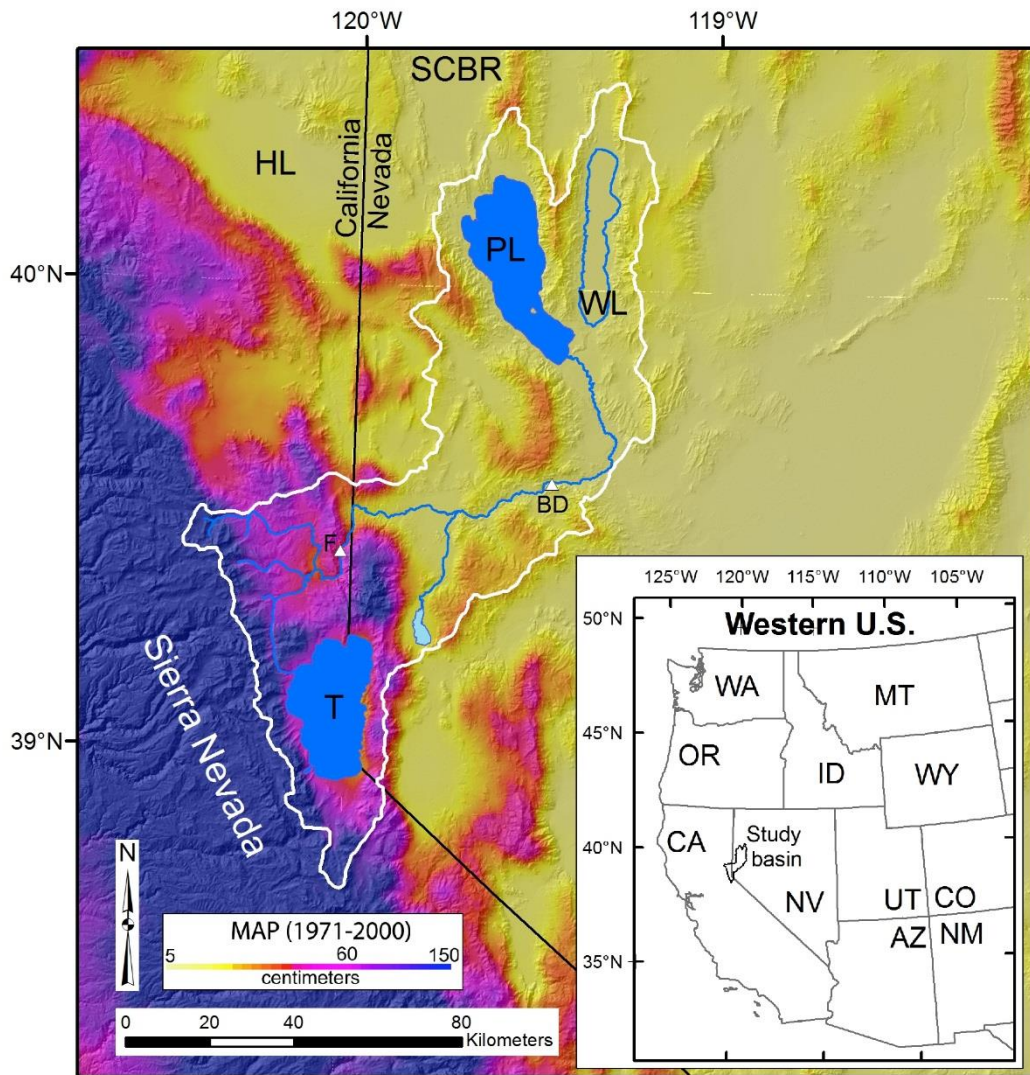


Figure 2

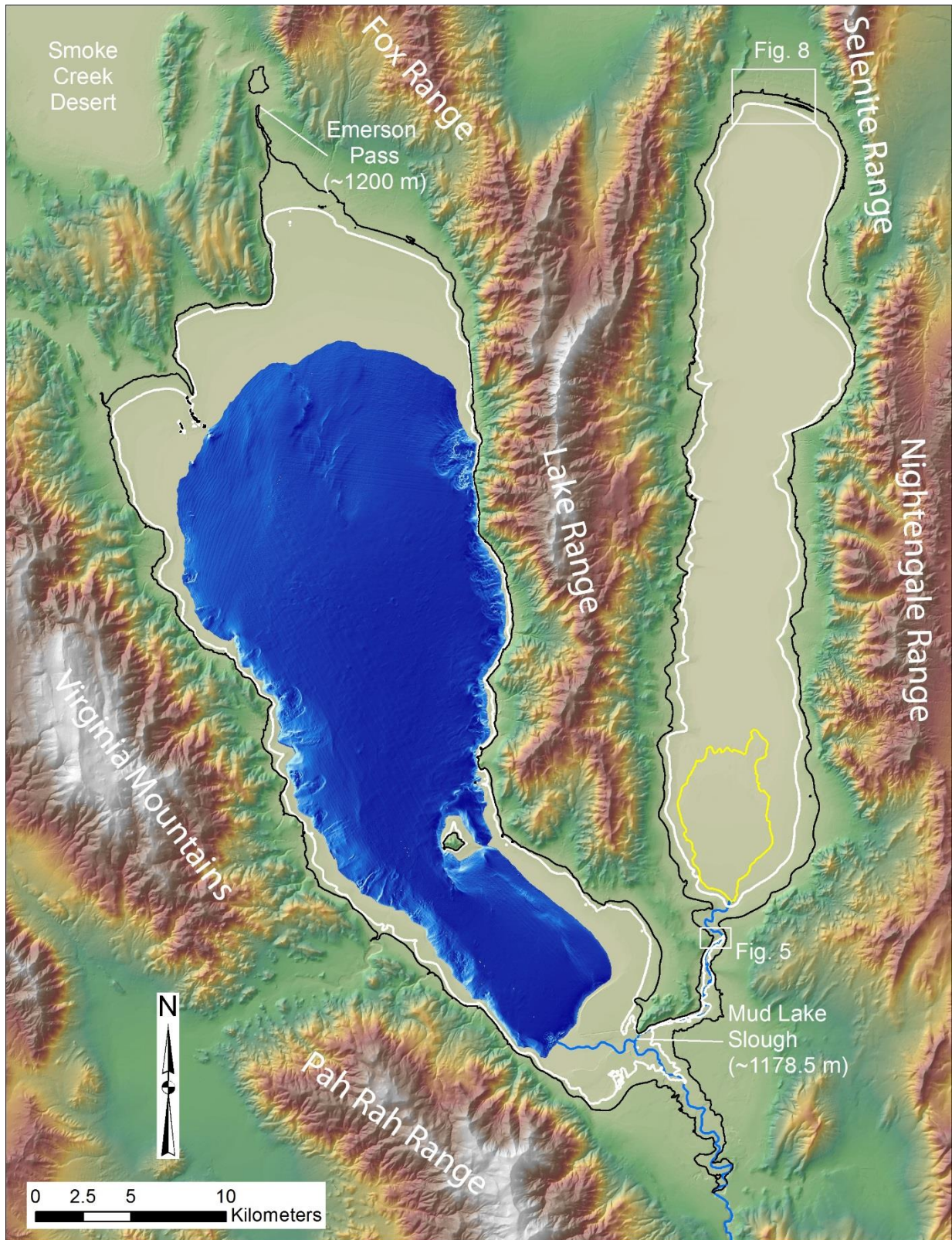


Figure 3

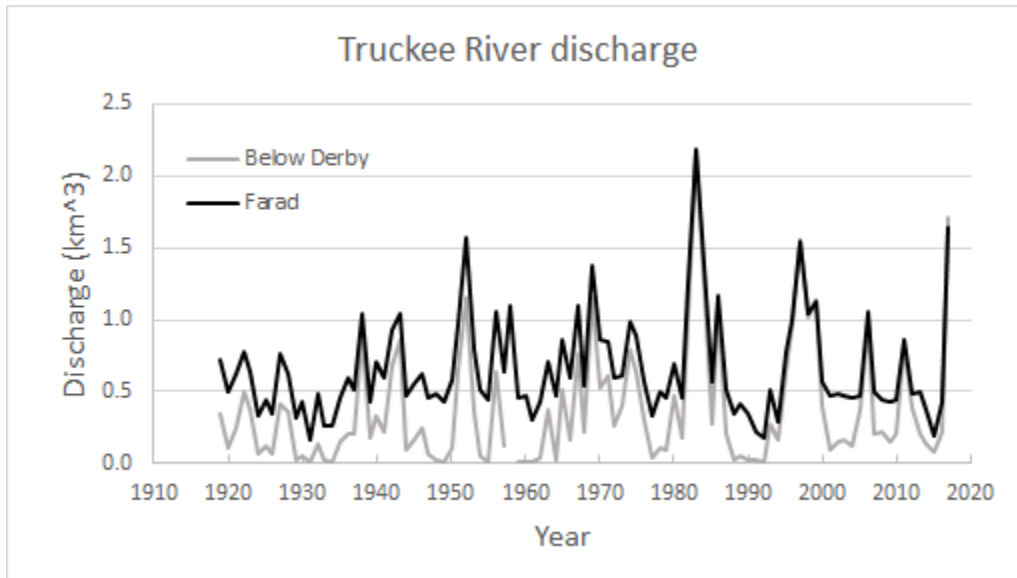


Figure 4.

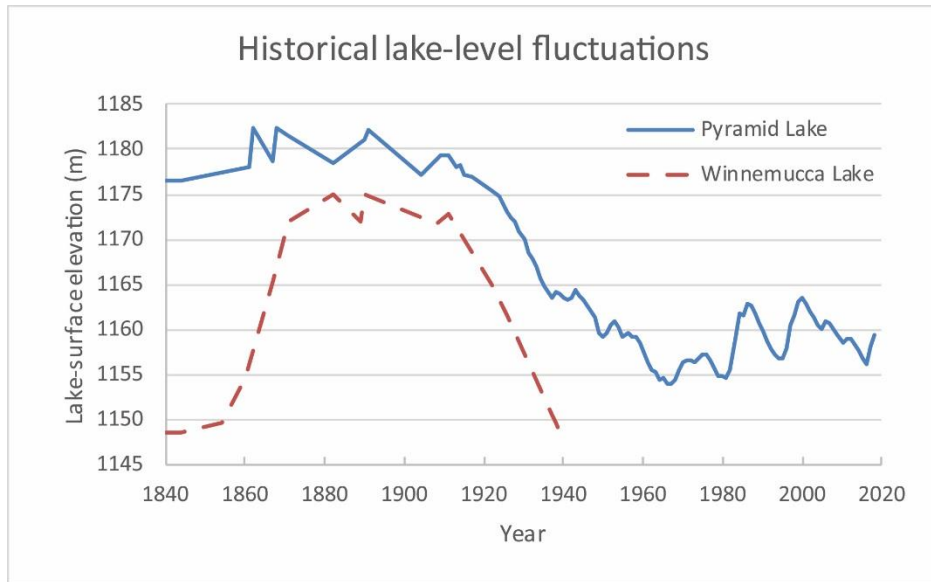


Figure 5

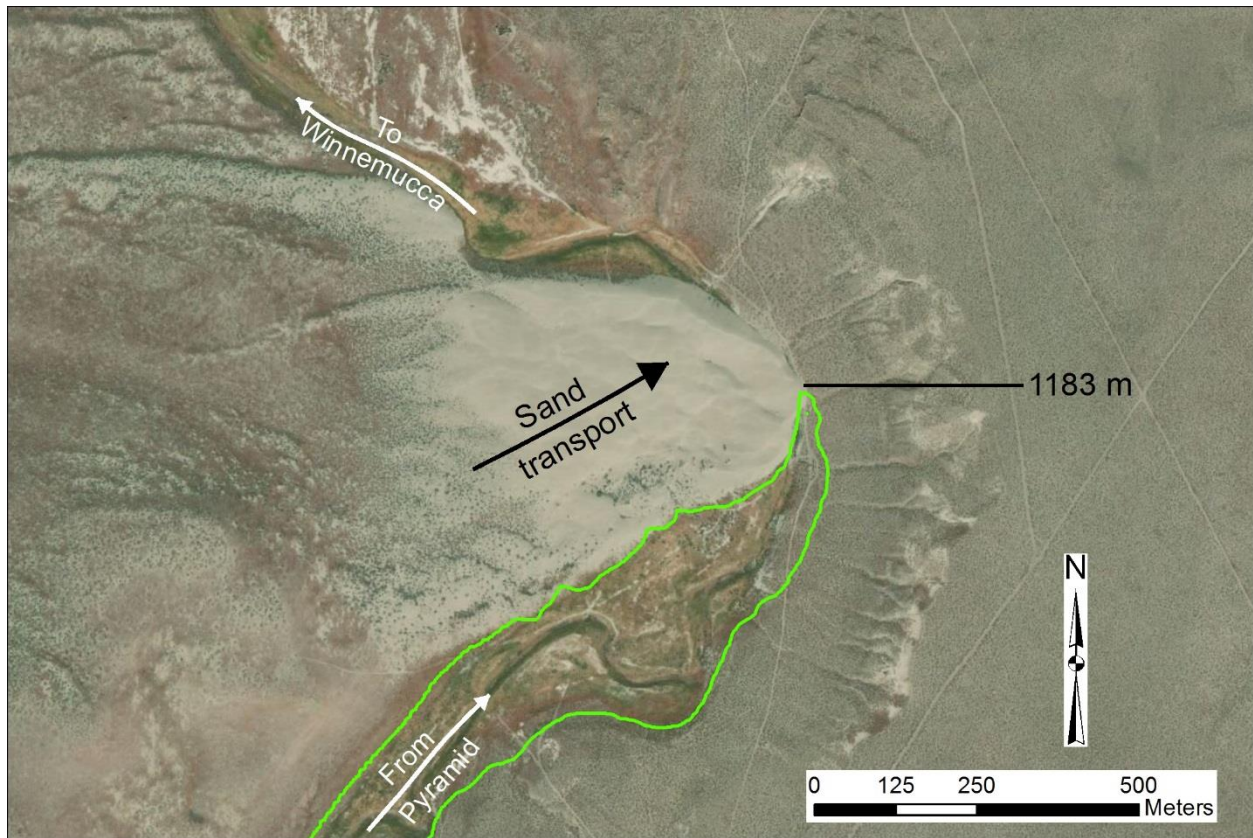


Figure 6

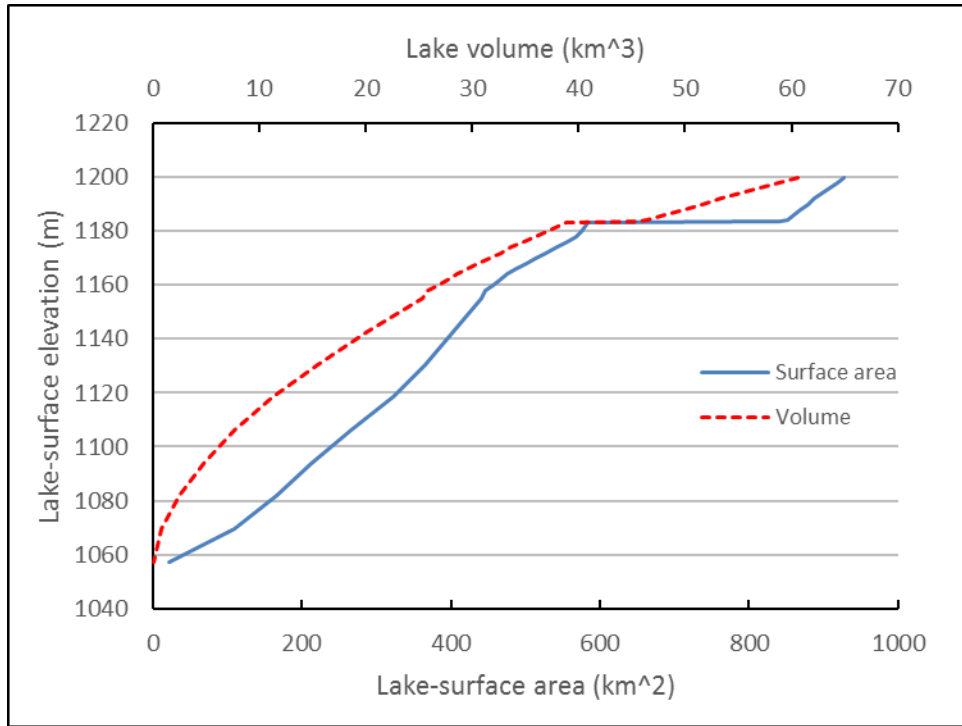
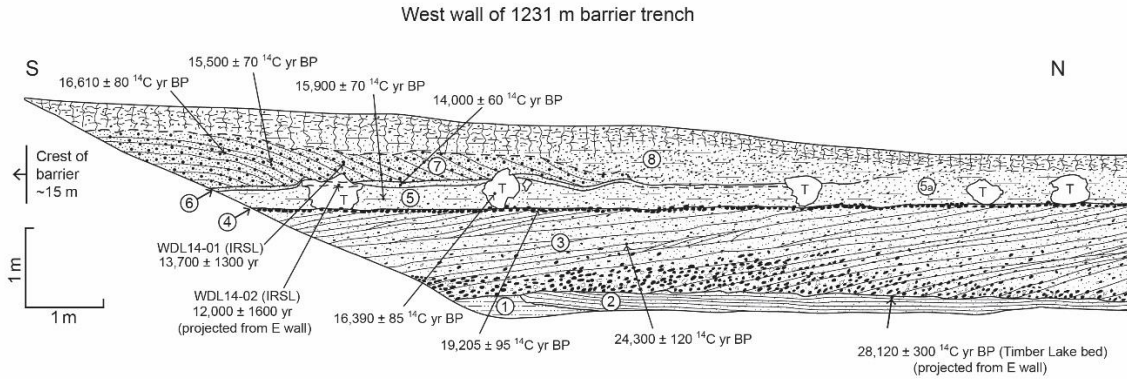


Figure 7



Trench log of 1231m barrier
 North end of Winnemucca Dry Lake
 UTM NAD83 11T 0301288 4465783
 Trench orientation: N-S

- | | |
|---|--|
| <p>⑧ Pebbly fine sandy-silt; heavily bioturbated</p> <p>⑦ Fine gravel and pebbles; primarily well-rounded volcanics</p> <p>⑥ Well-sorted, medium to coarse sand with abundant broken shells and chara</p> <p>⑥a Pebbly fine sandy-silt with zones of pebbles and gravel that suggest bioturbation</p> <p>⑤ Pebbly fine sandy-silt; large tufa heads contained within this layer (T)</p> | <p>④ Coarse well-rounded basaltic clasts capped by a thin semi-continuous laminar tufa layer</p> <p>③ Well-rounded to sub-angular gravel to pebbles to grit; primarily volcanic w/ occasional granitic clasts</p> <p>② Coarse granitic sand and grit</p> <p>① Dense, compact fine sandy silt</p> <p>Soil development T = Tufa</p> |
|---|--|

Figure 8

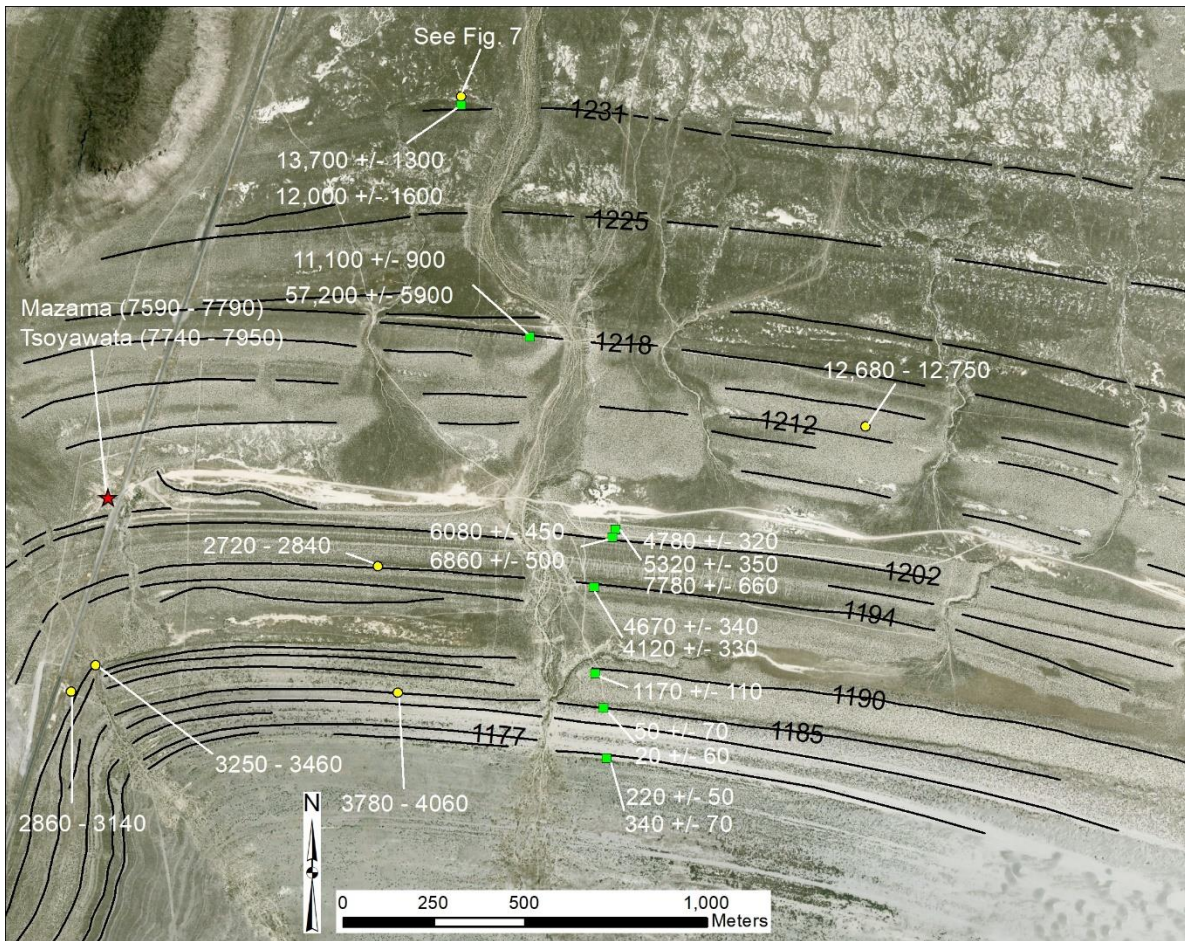


Figure 9

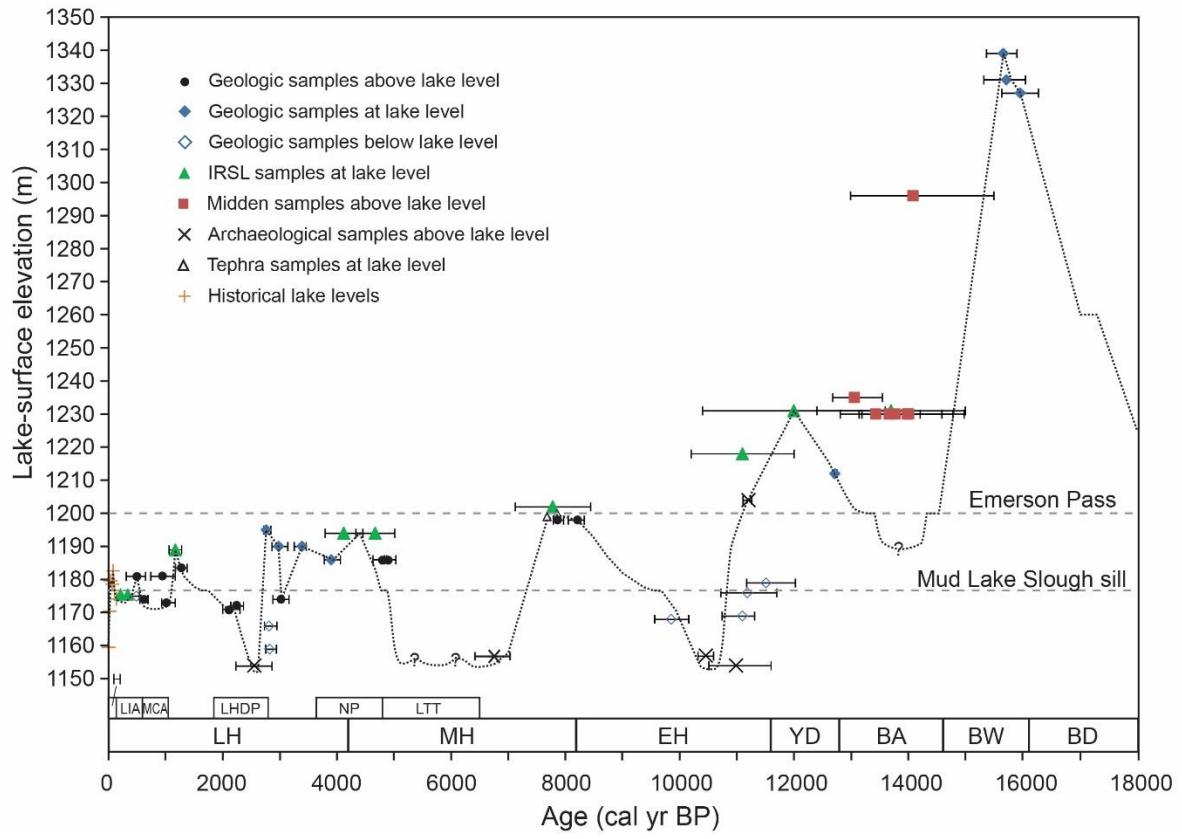


Figure 10

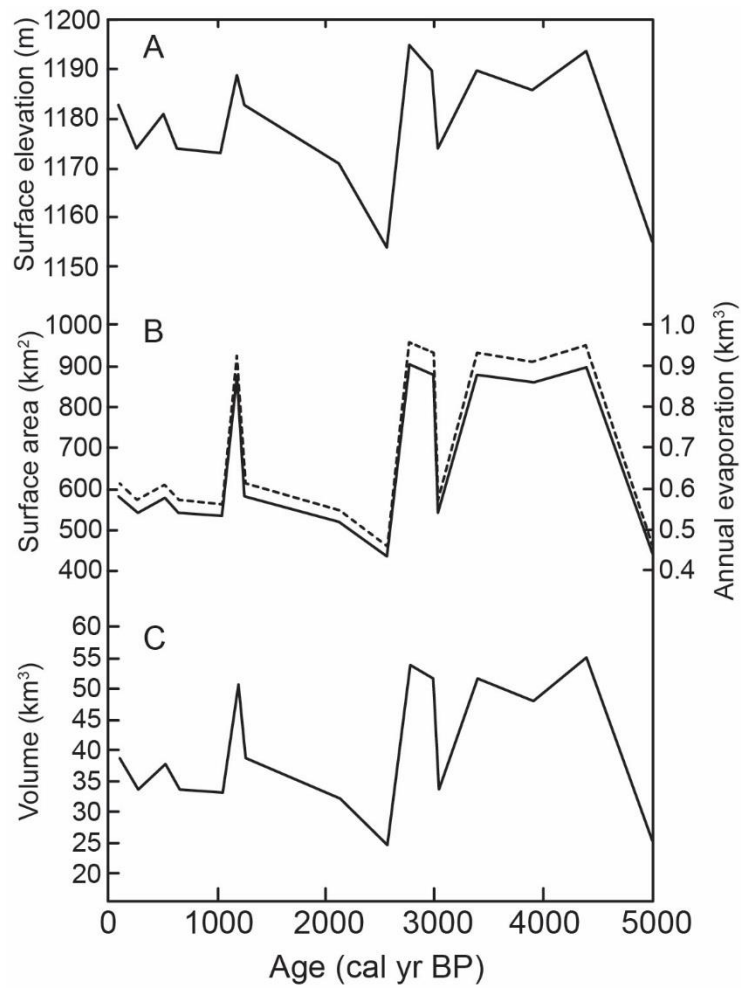


Table 1. Radiocarbon ages used to constrain lake-level fluctuations in the Pyramid and Winnemucca lake basins.

Setting or location	Sample #	Sample material	Age (¹⁴ C yr BP)	Age ^a (cal yr BP) (2σ)	Median probability	Elevation (m)	Relation to lake level	References
Delta deposits	Beta-202821	wood	430 ± 40	330-540	491	1175	below	Bell et al. (2005a)
Stream alluvium (Qty2)	GX-31721	charcoal	470 ± 90	310-650	501	1181	above	Bell et al. (2005a)
Stream alluvium	WIS-363	wood	670 ± 55	550-690	628	1174	above	Born (1972)
Stream alluvium	I-8195	wood	1025 ± 85	740-1170	940	1181	above	Prokopovich (1983)
Stream alluvium	WIS-364	wood	1110 ± 55	930-1170	1026	1173	above	Born (1972)
Stream alluvium (Qty3)	Beta-165927	pelecypod	1240 ± 40	1170-1300	1240	1183	above	Bell et al. (2005b)
Stream alluvium (Qty)	Beta-192176	charcoal	2130 ± 40	2000-2300	2112	1171	above	Bell et al. (2005a)
Stream alluvium	WIS-378	wood	2270 ± 55	2140-2360	2248	1172	above	Born (1972)
Wizards beach	GaK-2386	Sagebrush	2480 ± 120	2210-2840	2553	1154	above	Hattori and Tuohy (1993)
Beach ridge	CAMS-81201	charcoal	2635 ± 40	2720-2840	2760	1195	at	Briggs et al. (2005)
Delta slope	WIS-375	wood	2690 ± 65	2730-2950	2810	1166	below	Born (1972)
Delta slope	WIS-361	wood	2710 ± 60	2750-2940	2821	1159	below	Born (1972)
Beach ridge	Beta-180315	gastropods	2860 ± 40	2860-3140	2979	1190	at	This study
Stream alluvium	WIS-376	wood	2890 ± 50	2880-3160	3025	1174	above	Born (1972)
Beach ridge	Beta-174834	gastropods	3160 ± 40	3250-3460	3387	1190	at	This study
Beach ridge	CAMS-93340	gastropods	3595 ± 35	3780-4060	3901	1187	at	Briggs et al. (2005)
Alluvial fan	CAMS-88191	charcoal	4235 ± 40	4630-4870	4792	1186	above	Briggs et al. (2005)
Alluvial fan	CAMS-90557	charcoal	4320 ± 45	4830-5030	4896	1186	above	Briggs et al. (2005)
Wizards beach	GX-19421-G	bone	5905 ± 125	6410-7020	6734	1157	above	Edgar (1997)
Mazama tephra	NA	charcoal	6845 ± 50	7590-7790	7677	1199	at	Bacon (1983)
Tsoyawata tephra	NA	charcoal	7015 ± 45	7740-7950	7856	1200	at	Bacon (1983)
Pyramid Lake-Nixon Terrace (Qtn)	Beta-192174	charcoal	7020 ± 40	7760-7940	7863	1198	above	Bell et al. (2005a)
Pyramid Lake-Nixon Terrace (Qtn)	Beta-192173	organic sed	7380 ± 40	8050-8330	8211	1198	above	Bell et al. (2005a)
Pyramid Lake delta slope	WIS-374	wood	8800 ± 90	9560-10160	9853	1168	below	Born (1972)
Wizards beach	CAMS-28124, 29810, GX-19422G	bone	9273 ± 40 ^b	10300-10570	10457	1157	above	Tuohy and Dansie (1997); Edgar (1997); Adams et al. (2008)
Wizards beach	GX-13744	cordage	9660 ± 170	10510-11600	10985	1154	above	Tuohy (1988)
Pyramid Lake delta slope	WIS-377	wood	9720 ± 100	10740-11310	11097	1169	below	Born (1972)
Wallman bison	UCR-3782	bone	9779 ± 50	11110-11260	11204	1204	above	Dansie and Jerrems (2005)
Pyramid Lake delta	I-8194	wood	9780 ± 135	10720-11700	11186	1176	below	Prokopovich (1983)
Pyramid Lake delta	I-8193	wood	9970 ± 140	11170-12020	11512	1179	below	Prokopovich (1983)
Pyramid Lake beach ridge	CAMS-90412	pelecypod	10820 ± 35	12680-12750	12719	1212	at	Briggs et al. (2005)
Fishbone Cave	L-245	juniper roots	11200 ± 250	12680-13550	13062	1235	above	Thompson et al. (1986)
Guano Cave #11	A-3699	juniper	11580 ± 290	12810-14070	13433	1230	above	Thompson et al. (1986)
Guano Cave #7B1	A-3696	juniper	11810 ± 230	13140-14210	13667	1230	above	Thompson et al. (1986)
Guano Cave #6A	A-3695	juniper	11890 ± 250	13190-14590	13769	1230	above	Thompson et al. (1986)
Falcon Hill #2	A-3489	juniper	12020 ± 470	12990-15500	14084	1296	above	Thompson et al. (1986)
Guano Cave #10	A-3698	juniper	12060 ± 260	13410-14980	14008	1230	above	Thompson et al. (1986)
Guano Cave #9	A-3697	juniper	12070 ± 210	13460-14780	13984	1230	above	Thompson et al. (1986)
Lahontan highstand at Jessup*	NSRL-3014	bone	13070 ± 60	15370-15900	15667	1339	at	Adams and Wesnousky (1998)
Jessup (near highstand)*	ETH 12798	gastropods	13110 ± 60	15460-15980	15735	1331	at	Adams and Wesnousky (1998)
Jessup (near highstand)*	ETH 12799	gastropods	13280 ± 60	15750-16180	15968	1327	at	Adams and Wesnousky (1998)
1231 m beach ridge at WL	KDA040208-C2	ostracodes	14000 ± 60	16710-17240	17003	1230	at	This study
1231 m beach ridge at WL	KDA040208-C1	ostracodes	15500 ± 70	18600-18900	18761	1230	at	This study
1231 m beach ridge at WL	KDA040208-C3	ostracodes	15900 ± 70	18960-19420	19170	1230	at	This study
1231 m beach ridge at WL	KDA040208-C6	tufa	16390 ± 85	19550-20020	19781	1230	below	This study
1231 m beach ridge at WL	Beta-174833	gastropods	16610 ± 80	19780-20300	20042	1231	at	Adams et al. (2008)
1231 m beach ridge at WL	KDA040208-C4	tufa	19205 ± 95	22860-23460	23142	1230	below	This study
1231 m beach ridge at WL	KDA040208-C5	ostracodes	24300 ± 120	28000-28660	28341	1230	at	This study
Timber Lake tephra	NA	organic carbon	28,120 ± 300	31310-32840	31999	1229	at	Benson et al. (2003); This study

^aAll radiocarbon ages calibrated with Calib 7.1 using the IntCal13 calibration curve (Reimer et al., 2013).

^bAverage of three radiocarbon ages (Adams et al., 2008).

Table 2. Luminescence ages from beach ridges at the north end of Winnemucca Lake.

Field ID	Laboratory code	Easting ^a	Northing ^a	Beach ridge elevation (m)	depth (m)	K (%)	U (ppm)	Th (ppm)	Cosmic dose rate (Gy/ka)	Total dose rate (Gy/ka)		1 sigma uncertainty	Age (years before 2014)		1 sigma uncertainty
WDL14-01	J0693	301210	4465965	1231	0.94	1.0	4.63	5.50	0.23	3.11	±	0.13	12,000	±	1600
WDL14-02	J0694	301210	4465965	1231	0.68	1.9	3.46	6.60	0.24	3.73	±	0.20	13,700	±	1300
WDL14-03	J0695	301399	4465328	1218	0.76	2.9	1.45	4.10	0.24	4.08	±	0.28	11,100	±	900
WDL14-04	J0696	301399	4465328	1218	0.88	3.1	1.30	3.30	0.23	4.16	±	0.29	57200 ^b	±	5900
WDL14-05	J0697	301635	4464798	1202	0.31	1.3	3.21	6.00	0.25	3.13	±	0.15	4780 ^b	±	320
WDL14-06	J0698	301635	4464798	1202	0.50	1.2	3.73	5.70	0.25	3.13	±	0.15	5320 ^b	±	350
WDL14-07	J0699	301635	4464798	1202	0.87	1.1	4.04	5.70	0.23	3.11	±	0.13	7,780	±	660
WDL14-08	J0700	301626	4464776	1202	0.62	1.8	2.48	5.20	0.25	3.42	±	0.19	6080 ^b	±	450
WDL14-09	J0701	301626	4464776	1202	0.92	1.1	3.79	5.20	0.23	3.06	±	0.13	6860 ^b	±	500
WDL14-10	J0702	301575	4464640	1194	0.68	2.1	1.52	2.80	0.24	3.36	±	0.21	4,120	±	330
WDL14-11	J0703	301575	4464640	1194	0.40	2.0	1.74	2.80	0.25	3.33	±	0.20	4,670	±	340
WDL14-12	J0704	301578	4464402	1190	0.50	1.8	2.70	5.80	0.25	3.46	±	0.19	No yield		NA
WDL14-13	J0705	301578	4464402	1190	0.75	2.3	1.59	18.10	0.24	3.81	±	0.23	1,170	±	110
WDL14-14	J0706	301602	4464307	1185	0.86	1.5	3.05	6.30	0.23	3.30	±	0.16	50 ^b	±	70
WDL14-15	J0707	301602	4464307	1185	1.00	1.7	2.41	5.40	0.23	3.34	±	0.17	20 ^b	±	60
WDL14-16	J0708	301610	4464169	1175	0.34	1.5	1.64	6.60	0.25	3.14	±	0.18	220	±	50
WDL14-17	J0709	301610	4464169	1175	0.64	1.5	1.78	4.50	0.24	3.13	±	0.17	340	±	70
^a UTM coordinates are all in Zone 11 NAD83															
^b Ages not used in figure 9.															